Sandwich Plate Systems

The application of Sandwich Plate Systems as impact protection in offshore structures

P.C. Boersma

Master of Science Thesis

TU Delft Delft University of Technology

Offshore and Dredging Engineering

Sandwich Plate Systems

The application of Sandwich Plate Systems as impact protection in offshore structures

Delft University of Technology
Department of
Maritime and Transportation Technology

June 20, 2017

The thesis committee members that have read and recommend to the Faculty of Mechanical, Maritime and Materials Engineering (3mE) for acceptance of this thesis entitled

Sandwich Plate Systems

by

P.C. Boersma

in partial fulfillment of the requirements for the degree of

Master of Science in Offshore Engineering

are:

Supervisors:	Dr.ing. A. Romeijn
	Dr.ir. M. Witteman
Readers:	Dr.ing. A. Romeijn
	Dr.ir. G. Bufalari
	Dr.ir. M.Godjevac
	Dr.ing. G. Langerak

Faculty of Mechanical, Maritime and Materials Engineering (3mE) · Delft University of Technology

Abstract

During operations on offshore platforms, lifting of objects (i.e. containers) brings with it dropped object risks. In the occurrence of a dropped object event, production is temporarily interrupted, resulting in unintended costs. *Chicago Bridge & Iron Company* (CB&I), a leading engineering company in the design of offshore topside structures, is continuously seeking for innovative solutions which minimize costs. To date, protection of vulnerable equipment against dropped objects is provided by conservative stiffened steel plates. An alternative in the form of Sandwich Plate System panels has been researched, as it could potentially reduce costs due to their high failure load to mass ratio.

Multiple design thicknesses for simply supported Sandwich Plate System (SPS) beam and plate structures have been considered analytically and numerically. Their masses and failure loads when subjected to quasi-static loads have been compared with a Stiffened Steel Plate (SSP) reference structure. ANSYS, a Finite Element Analysis software package has been used to analyse the force-deflection curves associated with each design and to compare the plots and results with the results obtained analytically.

Analytical calculations of the bending moment resistance have shown to be adequate for the beam models under strict assumptions only. For more comprehensive non linear analyses including circular impact loads, an analytical analysis is no longer readily accessible and a numerical analysis is required. While for stiffened steel structures subjected to a line load a 'beam to plate' simplification assumption is justified, this is not the case for SPS due to its additional transverse stiffness. For beam structures subject to line or circular failure mechanisms, the SSP layout offers a greater yield resistance with respect to its mass than SPS. For plated structures subject to a circular failure mechanism the yield resistance increases more strongly for the SPS type, taking full potential of the increase in failure load through the additional transverse stiffness.

It can be concluded configurations of SPS with low face plate to core thickness ratios come closest to providing similar yield resistances as SSP, while maintaining a low mass. For the configurations investigated, SPS 5-45-5 seems to provide a best fit as a replacement for SSP-600, since the weight is lowest with respect to the minimum required yield resistance. No configurations for SPS are found to be better than SSP-600 when the models are considered 2D. For 3D models the additional stiffness in transverse direction significantly increases the maximum failure load of SPS. However, for the considered cases in this report no beneficial SPS configurations regarding yield failure were found.

Preface & Acknowledgements

Last year I have had the opportunity to complete my study by doing research on sandwich plate system structures; a promising structural plate layout for the protection of dropped impact events. During this period a great group of people offered their guidance and help in completing this thesis research. I would therefore like to take this opportunity to express my gratitude to those who did.

First of all I would like to thank my colleagues at CB&I and in particular Dr. Ir. M. Witteman for their input and persistent willingness to help, as well as offering me the opportunity to tackle a present industry related problem.

My gratitude also goes out to Delft Technical University, where in particular Dr. Ir. A. Romeijn, Dr. Ir. R. Bos and Dr. Ir. G. Bufalari have provided and shared their insights and knowledge on the subject, helping me greatly.

An honorable mention to my friends at the university, Piet, Bart & Arnela, who have morally supported me during solitary days at the university.

Last but definitely not least, I would like to thank my parents, Henk and Akke, who have always supported me unconditionally. Their contribution has undoubtedly been of importance towards the complementation of my thesis and I therefore dedicate my thesis to them.

Delft, University of Technology *P.C. Boersma*
June 20, 2017

Glossary

List of Acronyms

ABS	American Bureau of Shipping
APDL	ANSYS Programming Design Language
CB&I	Chicago Bridge and Iron
CLPT	Classic Laminate Plate Theory
c.o.g	center of gravity
DNV	Det Norske Veritas
DOP	Dropped Object Protection
FE	Finite Element
FEA	Finite Element Analysis
FEM	Finite Element Model
IE	Intelligent Engineering
PU	Polyurethane
SPAR	Single Point Anchor Reservoir
SPS	Sandwich Plate System
SSP	Stiffened Steel Plate

Table of Contents

List of Figures

List of Tables

Chapter 1

Introduction

1-1 General Background

The oil and gas industry is moving towards offshore production facilities as resources on land become more scare. A Single Point Anchor Reservoir (SPAR) is an example of such an offshore production facility. CB&I, an Engineering, Procurement and Construction company, has been asked to design the topsides structure of the *Aasta Hansteen SPAR*, a SPAR to be operated by Statoil in the Norwegian Sea.

For the design of SPAR topsides, weight is an important factor due to buoyancy requirements. In general a lower weight of the topside structure results in lower project costs. To keep offshore projects economically viable, a reduction in weight is continuously sought after.

Currently, Stiffened Steel Plates (SSP) are conventional in offshore topside design. These plates serve as deck plating while also offering protection to vulnerable equipment against dropped impact loads. Previous research by Intelligent Engineering [1] - manufacturers of Sandwich Plate Systems (SPS) - has shown that it is possible to reduce the weight of deck plating by up to 20% using SPS instead of SSP. To date SPS is commonly known from their use in the aviation industry and expansion to the offshore industry is an interesting topic.

SPS structures are sandwich plates existing of multiple materials. Although variants of SPS exist, a specific SPS layout composed of two steel face plates and a polyurethane elastomer core is considered in this research. The configuration of these plates is shown in Figure 1-1. Due to the polyurethane core, the structural layout of SPS offers a variety of advantages. The reduction in weight is realized by the low density of the core layer. Simultaneously SPS remains stiff having a high flexural rigidity through the distance of the face plates to the neutral bending axis. Additionally SPS seems to offer a better fire- and impact resistance than regular steel stiffened plates [2],[3], all while simplifying the construction by eliminating the use of stiffeners. Whether the use of SPS is more cost beneficial than SSP as a deck impact protection structure on offshore topside facilities has been researched in this report.

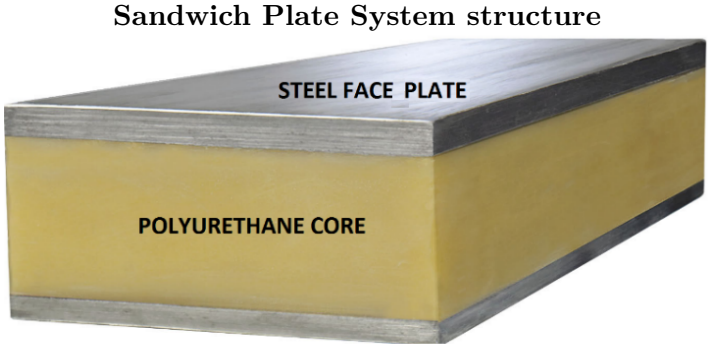

Figure 1-1: SPS configuration; two steel face plates and a polyurethane core

1-2 Previous work

Previous research, ranging from general plate theories to SPS structural design, have been studied. The study included theory on the failure modes of SPS, plastic material deformations and plate impact response for plates subjected to low impact velocity loads. The extensiveness of the study has been limited by taking into account the Classic Laminate Plate Theory (Kirchhoff) only.

Plantema [4], Allen [5] and Zenkert [6] have summarized the literature on sandwich beams, which includes a systematic stiffness and strength design strategy for SPS structures. For minimum weight design, generally failure mode maps are constructed, often related to a function of the appropriate structural load. Given a certain loading, an expected failure mode for the structure is determined from these maps. The governing failure modes for SPS structures loaded in bending are recognized by Gibson and Ashby [7]. The governing failure modes are either face yield, core shear, indentation or a combination of those, dependent on the material properties, the face plate to core thickness ratio and the width to length ratio of the plate. *Figure: 1-2* provides an example of such a failure mode map, where the axis indicate the previously mentioned ratios.

A multitude of failure mode maps for SPS beams subjected to static bending loads have been constructed by C. Steeves & N. Fleck [11]. Their research indicates the failure mode, associated with the applied loads and plate structures of the cases considered in this report, is likely yielding.

Yielding, which is in many cases the governing failure mode for *statically* loaded plates subjected to bending, has been researched quiet excessively. The associated plastic behaviour of regular plates is explained by A.C.W.M. Vrouwenvelder [8] in the form of failure mechanisms.

Y. Yuan & P. Tan [9] investigated the failure modes of clamped steel plates subjected to impulse loading. They found that for *dynamic* loading the failure mode of plates is not only dependent on its geometry and boundary conditions, but also on the impact velocity. During their research a distinction was made between yielding and other failure modes, where for yielding the impact velocity remained below a certain critical value (the critical impact velocity). This phenomenon is explained by material damping and energy dissipation, which invoke a decaying response of the elastic waves generated by the impact loading. The duration of impact therefore plays a key role in determining the type of impact response.

Example of a failure mode map; SPS beam structure

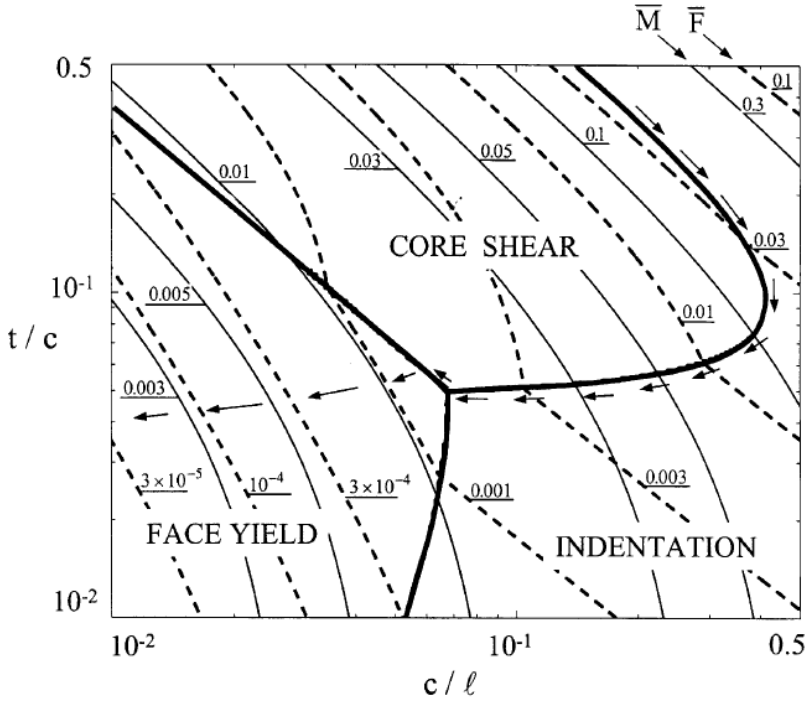

Figure 1-2: Example of a SPS beam structure failure mode map. The governing failure modes are; face yield, core shear or indentation.

N.Razali et al. [10] reviewed impact damage on composite structures, distinguishing impact loads by their impact duration. They concluded that dropped impact loads usually are associated with impact durations longer than the time required for the waves to reach the structures boundaries, resulting in a quasi-static response.

Besides theoretical studies, experimental tests have previously been carried out by multiple parties. *S. Teixeira de Freitas* [12] has conducted several test and finite element verification studies on SPS beams subjected to static bending loads. Intelligent Engineering [2] put emphasis on impact loads, consolidating their findings with Finite Element Analyses. As the manufacturers of SPS, their suggested engineering guidelines towards material properties and Finite Element Analyses have been taken into account. Finally, the design criteria and analyses in this report are bound to the rules and regulations presented by leading classification societies, e.g. Det Norske Veritas [13]. Requirements and regulations by *CB&I* have been taken into account as well.

1-3 Problem definition

The current impact protection of the *Aasta Hansteen* topside structure seems to bring with it unnecessary costs due to excessive weight. For protection against damage from dropped objects stiffened steel plates are used, which simultaneously function as deck plating. This design (*Figure: 1-3a*) seems suboptimal compared to the alternative solution provided in the form of SPS structures (*Figure: 1-3b*). To stay competitive and to be able to offer clients the

best solution, optimization of the costs for future topside structure design is essential. So far, insufficient knowledge on SPS structures subjected to dropped impact loading has prevented CB&I from using these plate designs. Research towards the use of SPS as an impact protector is therefore required.

Different deck plating design possibilities

(a) Cross sectional area of stiffener **(b)** Cross sectional area of the sandwich

Figure 1-3: Optimal design: Stiffened Steel Plate versus Sandwich Plate System structures

1-4 Scope

The scope of this research contains the assessment of impact loading on SPS structures. The aim is to get a better understanding of impact behaviour on SPS structures, and to ultimately decide whether they are a viable alternative to the stiffened steel plates used currently.

The non-linear behaviour of plates during impact excludes analytical solutions from being conclusive and makes a Finite Element Analysis a requisite. Different topics related to impact behavior of the plate structures have therefore been taken into account;

- Dropped object event scenario
- Assumptions and framework
- The yield failure mode and the associated failure mechanisms
- Preliminary design; mass and bending moment resistance
- Plate impact response; impact duration and Eigen frequency

Results and conclusions about these topics are searched for via an analytical- and a numerical study. The analytical study serves as verification and helps with the preliminary design of more simple models, while the numerical study focuses on the more complex cases. ANSYS (a Finite Element Analysis program) is used to run scripts related to the impact loads on the chosen structures. The following ANSYS topics are considered;

- Modeling of the SSP and SPS structures
- Load implementation
- Element mesh convergence study

The input parameters associated with these topics are studied. First the SSP reference structure is considered, providing input for the plate model cases. Data by *Intelligent Engineering SPS* [14] is used to value material properties and plate boundary conditions.

Normally, experiments are carried out to validate the results of the FEA and to get an even better understanding of the plate impact behaviour. However, due to the considered cases, experiments would be too expensive and time consuming. Validation of the FE analyses is therefore provided by comparing the numerical results with previous research on SPS structures.

1-5 Objectives

The goal of this research is to find an optimal (cost-effective) solution for protection against dropped impact loads. This is done by comparing the impact resistance of different plate types subjected to impact loading when the yield failure mode is governing. SPS structures are compared with conventional stiffened steel deck plating currently considered for the design of the *Aasta Hansteen* SPAR topside facility.

The search for a minimum SPS deck plate weight design leads to different structural layouts being considered. The found thickness configurations should directly or indirectly ensure that the total costs of the project are reduced compared to the conventional SSP design. To meet these requirements the following objectives are set;

Research & Preperation

- Research scenario study
- Case definition
- Analytical study

Pre-processing; FEA analysis (ANSYS)

- Modeling of the plate structures
- Load simulation of dropped object

Post-processing; Validation & Optimization

- Compare analytical and numerical results
- Find an optimal configuration for SPS structure
- Interpretation of the results

After completion of these objectives an answer to the main question of this research should be found:

Are steel-polyurethane-Sandwich Plate System structures a viable alternative to stiffened steel deck plating for the protection of offshore structures from accidental dropped object loads?

1-6 Thesis Outline

This thesis report has been structured in a chronological order, with each chapter defining a specific part of the research. Appendices have been added to provide additional information on certain aspects within the chapters or to provide relevant information which is not directly related to the research but nonetheless important to the conclusions drawn in the final chapter.

In *chapter 2* an introduction is given to the general approach for studying dropped object impact. A strategy to finding an optimal solution is evaluated and a work frame is set for the given problem.

Analytical formula and associated assumptions for beam like structures are presented in *chapter 3*. Preliminary conclusions are drawn from calculations made and provide an idea of the SPS thickness configurations to be used during the numerical analysis.

In *chapter 4* SPP and SPS finite element models are constructed which represent the practical designs. Associated with the design are the boundary conditions, the applied loads, the considered element types and its meshing.

Chapter 5 includes a numerical analysis of simply supported beam and plate SSP and SPS structures subjected to circular quasi-static loading. A comparison is made between the failure loads and the maximum deflection. Additionally, the impact duration range for which a quasi-static loading assumption is viable has been determined. For loads outside this range transient analyses are conducted.

Finally, in *chapter 6* an overview of conclusions found from the analytical and numerical studies is presented. A decision is made on which plate design is optimal against dropped object impact loads for offshore topside structures.

Chapter 2

Research Methodology

The research methodology describes the general process or approach of reaching the objectives mentioned in *Chapter 1*. A conducted strategy evaluation is persisted as a guideline for the general approach of this research. A large component of the strategy evaluation is carrying out an impact assessment, a comprehensive task elaborated in *paragraph 2-2* of this chapter.

2-1 Strategy Evaluation

This research has been separated into two main phases, following the approach used by DNV-RP-C204 for the structural response analyses of individual components. This approach exists of two methods.

- Analytical approach; an approximation of the static solution
- Numerical approach; a non-linear finite element analysis

The analytical approach has been considered as a preparation phase ('Phase 1'), while the numerical approach has been considered as an impact analysis part consisting of two phases ('Phase 2a' and 'Phase 2b'). Phase 1 involves preparations necessary to conduct the numerical analyses executed in Phase 2. This includes the impact assessment, analytical study and the numerical modeling of the structures. Phase 2a and 2b are both numerical impact analysis phases. The first part includes the impact analysis of stiffened steel plates. The second part deals with the impact analysis of SPS structures. Both parts include beam- and plate-model configurations to show the effects of the length to width ratio of the model, as well as the effects of different failure mechanisms.

Phase 1: Preparing the analyses

- Impact assessment & framework

- Set analysis assumptions and boundary conditions
- Analytical study; preliminary design
- ANSYS Modeling

Phase 2a & Phase 2b: Numerical impact analyses of SSP & SPS structures

- step 1; Linear material, static load analysis SSP & SPS beams (not presented)
- step 2; Non-linear material, static load analysis SSP & SPS beams
- step 3; Verification of models
- step 4; Linear material, static load analysis SSP & SPS plates (not presented)
- step 5; Non-linear material, static load analysis SSP & SPS plates
- step 5; Validation of models
- step 6; Conclusions & recommendations

In the first phase an analytical comparison is made between the elastic and plastic section moduli of the SSP reference structure and a range of SPS thickness configurations. Based on this study a limit is set to the minimum and maximum thickness of the SPS design and an estimate is made on which SPS thickness configurations could serve as most optimal.

Subsequently, during the second phase a numerical comparison is made between the maximum dissipated energy for the SSP model and the limited range of SPS thickness configurations. The maximum dissipated energy is determined from force-deflection graphs, which provide the deflection and maximum external load resistance of the plate. By limiting the deflection of the plate based on the accidental limit state (ALS) design criteria for SSP and SPS, either in the form of maximum strain or a ductility ratio, the maximum dissipated energy is found. Among the SPS configurations that exceed the maximum dissipated energy of SSP an optimization is made based on the minimum weight.

The numerical analysis is executed in accordance to 'impact loading assessments' as described in DNV-RP-C208. The finite element analysis is executed using ANSYS. Using the APDL a script is written for each considered case, from which it is possible to quickly adjust various conditions like material properties, structural geometry and load conditions.

Additional information regarding advertised installation, maintenance and fire resistance benefits of SPS are provided in *Appendix: B*. Although these properties are not the focus of this research, they may lead to application limitations in the offshore industry.

For completeness of the dropped object analysis assessment, damage as a result on the global structure should be considered as well [15]. Regardless, this part has not been included in the scope of this research since the impact loads seems unlikely to cause any permanent damage to the global structure.

2-2 Plate Impact Assessment

The general procedure considered by DNV RP-C204 and the American Bureau of Shipping (ABS) on how dropped object plate impact assessments should be conducted is followed. This procedure concludes two topics within the dropped load impact assessment which should be defined;

- The accident acceptance criteria
- The dropped object event

2-2-1 Accident acceptance criteria

The design acceptance criteria define the permissible amount of damage present in the system so that the risk levels for the facility can be assessed during and after the dropped object event. When structures are designed against impact loads and expected to exceed the elastic load capacity, the accidental limit state (ALS) is considered.

The ALS design of plate structures is governed by their critical deflection limit to avoid damage to process equipment. This critical deflection is often expressed as the maximum ductility ratio μ. The ductility ratio is a function of the maximum displacement of the structure, divided by the maximum elastic displacement of the structure at any given point. For the design against impact damage on the Aasta Hansteen SPAR topside facility, a maximum allowable ductility ratio of $\mu = 5$ has been chosen.

The ductility ratio may not be a proper failure criterion for SPS due to the large deflection before plastic deformation, which depends on the total thickness of the chosen configuration. The thinnest configurations in particular might exceed the maximum deflection for which the assumption of small angular deflections is no longer viable. Additionally the large deflection could result in underlying systems being damaged. Therefore the ALS maximum deflection limit for SPS is set similar to the maximum strain in the SSP structure at a ductility ratio of $\mu = 5$.

2-2-2 Dropped object event

The aim of a dropped object event scenario is to describe the given impact case as accurate as possible. Distinction is made between four primary inputs:

- A description of the dropped object event scenario
- Structural geometry
- Material properties
- Applied loading

These primary input parameters are discussed in the third chapter and are based on the dropped object event considered by CB&I.

2-3 Framework

To prevent excessive research, the framework section of this report lists the boundaries in finding answers to the given objectives mentioned previously.

- This research has been specified towards deck plating design. After a preliminary impact study by CB&I, the deck plating strength of laydown area #7 of the Aasta Hansteen had shown to be inadequate with respect to puncture.
- This research focuses on the yield strength analysis of plate structures. Exceedance of the design acceptance criteria follows from a numerical study. The maximum ductility criterion, as well as the maximum critical strain are based on requirements set by CB&I.
- The ductile design principle is used regarding the distribution of strain energy dissipation. This implies plastic deformations of the impacted structure, but no deformation of the impacting structure. This is in line with the general assumption of infinitely rigid impacting structures for dropped object studies [13]. The following requirements are met;
  - The ratio of ultimate failure load over yield failure load is greater than 1,1.
  - The ductility ratio of the failure material, defined as the ratio of the ultimate strain over the yield strain, is greater than 15.
  - The ultimate strain limit is greater than 15% or $\epsilon_u = 0,15$.
- The governing failure mode is yielding of the steel face plates. Other failure modes are neglected as they are not considered relevant for low velocity impact loads.

2-4 Assumptions

To make the project more manageable, assumptions are set to reach the objectives via small steps. Basic principles are researched first, extended by less restrictive theories later in order to obtain a more realistic answer.

2-4-1 Assumptions regarding the materials of SPS structures

- The top and bottom layer, as well as the core of the plate are isotropic and homogeneous.
- The damping properties of the visco-elastic core are neglected.
- Despite polyurethane having a strong strength-temperature dependency, temperature associated effects have been neglected. The temperature is assumed to not change significantly during and after impact.

2-4-2 Assumptions regarding the structural layout of the plate

- The thickness of the face plate layers are considered thin compared to the core's thickness. A face plate to core thickness ratio of 0,5 is considered as a maximum.
- The thickness of the plate is considered less than one-tenth of the span L of the plate (L/h>10).
- The costs of SPS per unit weight are assumed higher than the costs of SSP per unit weight. The maximum thickness of the SPS structure is limited by its weight.
- The minimum thickness of the SPS structure is limited by requirements set by Lloyd's register [16]. Lloyd's register requires any SPS structural design to have a minimum total thickness 21 *mm*. The minimum thickness for the polyurethane core is 15 *mm*, while both faceplates require a minimum thickness of 3 *mm*.

2-4-3 Assumptions regarding the structural properties

- The SPS structures are assumed to have symmetric faceplates perfectly bonded to the foam core. This eliminates the debonding failure mode.
- The maximum deflection of all structures is determined based on the Euler-Bernoulli beam theory.
- Small deformations and linear terms of strain-displacement relationship theories are assumed.

2-4-4 Assumptions made regarding structural failure

- Face yielding is the dominant failure mode for SPS structures subjected to impact loading.
- The structure has failed under impact loading when it has deformed 5 times the maximum elastic deflection or when the deflection of the SPS structure causes a strain similar to the strain at $\mu = 5$ for SSP structure.
- There is a perfect continuity at the interfaces and no slippage occurs while the plate is bending; i.e. displacements remain continuous at the inter-faces between the face plates and the visco-elastic core.

Chapter 3

Analytical study

This chapter discusses the analytical impact design formula for both SSP and SPS. The elastic and plastic section moduli are considered to provide a way of validating the numerical models and to draw a preliminary conclusion on which SPS thickness configurations could be viable as a alternative to SSP. For the stiffened steel plate a single design is considered, namely the one currently used for the Aasta Hansteen SPAR project. For SPS a range of designs is considered based on rules and regulations, bending moment resistance and mass.

In advance of determining the elastic and plastic bending moment formula, a transition from the physical model to the analytical model is considered by describing the material characteristics and calculation considerations.

3-1 Material characteristics and analytical considerations

A transition from the considered physical model to the analytical model is required to make calculations using existing plate theory equations. Interpretation of the analytical results shall be related to the choices made during this transition.

- ***Homogeneous* - Inhomogeneous;** a material is considered homogenous when its material properties are not a function of the position and thus hold the same values everywhere. It does not show irregular values or discontinuities, in contrast to inhomogeneous materials.
- ***Isotropic* - Orthotropic - Anisotropic;** a material for which the moduli do not depend on the direction in which the load is applied is said to be isotropic. For orthotropic or anisotropic materials the strength/stiffness-properties depend on the direction in which they are measured, e.g. the stiffness in x-direction and y-direction are different.

SPS is a structural composite material comprising two metal plates bonded with a polyurethane elastomer core. The SPS structure should be considered an isotropic, homogeneous material [14].

- **Elastic - Plastic;** fully elastic materials will return to their original state after unloading under any given force. In reality, especially under impact loading, a material often experiences local plasticity. Plasticity describes the situation when deformation of a material results in non-reversible changes of shape in response to the applied forces. A material is considered to have deformed plastically when the yield strength is exceeded.

  After reaching the yield strength, the material will not deform linearly with respect to an increase in load any longer. Often, due to strain hardening, the material strengthens at the loaded area and experiences yield changes. This results in a higher required stress to keep deforming the material. When no strain hardening is taken into account the material is said to be elastic perfectly-plastic. Under this assumption the yield strength of the material remains equal under an increase in loads and redistribution of moments is implied.

  The yielding of a material, in combination with the strain it experiences under loading can be represented by a stress-strain curve, which indicates the total energy that can be absorbed before the material fails. The assumption of elastic perfectly-plastic materials is a conservative choice.

The model's materials are considered as elastic perfectly-plastic, having bilinear strength-strain curves.

- **Von Mises;** The Von Mises failure criterion is often used to describe the yielding behaviour of isotropic materials (mainly steel or aluminum). When adjusting the plastic bending moment with a correction factor or by using the transformation method it is possible to apply Von Mises for SPS structures.

The Von Mises failure criterion seems to fit this analysis due to treating failure criteria from an energy perspective. Combined with the steel face plates being a ductile material, this failure criterion provides an accurate description of the yielding behaviour of the SPS structure.

- **Lower bound theorem - *Upper bound theorem*;** 3 solution techniques can be distinguished when theories for plasticity are considered. For analytical studies two of these techniques are of interest.
  - The lower bound theorem; based on equilibrium equations and satisfying the condition that stresses are not larger than the equivalent yield at strain.
  - The upper bound theorem; based on failure mechanisms obtained from yield line patterns.

  The latter is also known as the yield-line theory, from which a solution can be obtained using the principle of virtual work. This theory dictates an exact solution to the load capacity of the plate, by indication of a failure mechanism and a permissible stress field. However, it is not possible to determine deflections of the structure required for calculations regarding dissipated energy.

For the analytical study the upper bound/yield line theorem is used to find a yield line pattern and associated a failure load.

- **Finite strain - *Infinitesimal strain*;** finite strain (large deformation theory) deals with deformations in which both rotations and strains are arbitrarily large. Infinitesimal strain (small deformation theory) deals with deformation in which the displacements of the material particles are assumed to be much smaller than any relevant dimension of the body.

For the yield line theory to be applicable, geometrical non-linear effects are neglected and infinitesimal strain is considered. The constitutive properties of the material (such as density and stiffness) at each point are assumed to be unchanged by deformation.

- ***Boundary controlled response* - wave controlled response;** N. Razali [10] distinguishes between 2 types of plate impact response; boundary controlled and wave controlled response. The distinction is made based on the impact duration and Eigen period of the impacted structure.

  The impact duration can be divided in low and high velocity impact. Low velocity impact occurs when the contact time of the impactor is longer than the time of lowest Eigen mode of the plate. In such case, the support conditions (boundary conditions) are important as the stress waves generated outward from the impact point have time to reach the edges of the structural element, causing its full-vibrational response.

  In the case of dropped weight loading, where the impact velocity is low and the impacting mass high, a greater contact time is usually observed. This results in a boundary-controlled impact response, which allows quasi-static analytical calculations.

For the analytical study the plate impact response is considered boundary controlled. Calculations shall be interpreted as a result of quasi-static loads.

- **Temperature dependent - *Temperature independent*;** Different operational temperatures results in a variance of the material properties, mainly the yield strength. Higher operating temperatures result in a lower yield strength of polyurethane, reducing the stiffness of SPS panels. Teixeira [12] identified a significant change for a temperature range between -10 and 50 C.

Regardless of the strong influence of temperature variations, the materials are considered having fixed yield strengths. As the Aasta Hansteen will operate in a cold environment, the assumption of material properties at room temperature is a conservative choice.

3-2 Dropped object event scenario

The feasibility of the dropped object impact study has been ensured by a well-defined dropped object event scenario. A preliminary study by CB&I has indicated a particular area of the

Aasta Hansteen topside design needs further investigation. This area, 'Laydown Area #7', is subject to dropped object risks during production, in which the worst case scenario covers containers of 10.000 kg being dropped from 10 m. Other important factors related to the dropped object event, like the plate's impact response, - dissipated energy, - failure mechanism and - geometry are are considered similar for both the SSP and SPS structure as well.

3-2-1 Plate response

Let's once more consider the plate's impact response, which directly influences the analytical approach to impact design. Det Norske Veritas (DNV), a leading classification agency in the development of marine structures, indicates quasi-static impact response as one of 3 valid alternatives to determine dropped object effects. An example of boundary controlled, quasi-static impact response, as opposed to wave controlled response is shown in *Figure: 3-1a and 3-1b*. One may notice the load and deflection for boundary controlled impact response are largest at a similar time interval, emphasizing only a single time interval is of interest.

Different deck plating design possibilities

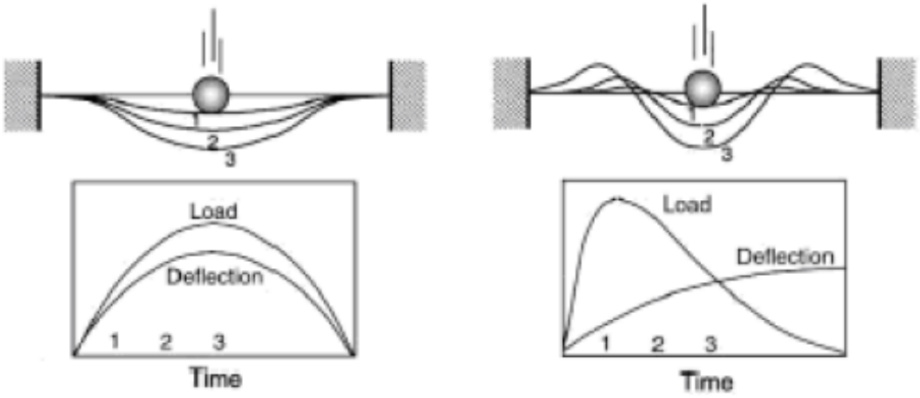

(a) Boundary Controlled Impact Plate Response

(b) Wave Controlled Flexure and Shear Waves Impact Plate Response

Figure 3-1: Plate Impact Response: Boundary vs. Wave Controlled

The maximum dropped impact duration to justify the use of boundary controlled quasi-static impact response is determined via numerical calculations of the Eigen period of the plates. To the best of the writers knowledge, the impact duration, being dependent on many independent variables, is difficult to determine by calculations. Exceedance of the Eigen period is therefore often determined via experimental research. Since this research report does not include experimental testing, previous research of plates with similar thicknesses is used to determine the impact durations.

3-2-2 Plate energy dissipation

With the assumption of quasi-static plate response, a limit can be set to the maximum energy dissipated by the plate. The total dissipated energy is bound to the boundary conditions of

the plate and its maximum deformation δ. The principle of virtual work combines these factors via a failure load $F_{failure}$, *Equation 3-1.*

$$W_{dissipated} = F_{failure} \cdot \delta \qquad [J] \tag{3-1}$$

Here, the failure load is a function of the failure mode, which (for yielding) depends on a failure mechanism and the bending moment resistance of the plate. The minimum energy dissipated by the plate is determined according to the kinetic energy equation, *Equation: 3-2.*

$$W_{dissipated} = E_{Potential} = m_{do} \cdot g \cdot h \quad [J] \tag{3-2}$$

3-2-3 Plate failure mechanisms

The plate's failure mechanism is a representation of how a structure will plastically deform when subjected to loading, given certain load- and boundary conditions. Each failure mechanism provides the relation between externally applied loads and the internal bending moment resistance of the structure via a length over which yielding takes place.

For statically determinate structures like simply supported beams subjected to loads at its center, the length over which yielding takes place is equal to the width of the beam. The relation between the applied load and bending moment may then indirectly be graphically presented via a force-deflection curve, see *Figure 3-2.* Initially the applied external load F is resisted by a linearly increasing internal bending moment resistance M_b up to first plastic deformation (*Figure 3-2*: point A). When plastic deformation of the structure has started a portion of the bending moment resistance increase is lost and the structure starts to deform non linearly (*Figure 3-2*: line A-B). For the purpose of analytical calculations this section is assumed bilinear, resulting in a simple resistance curve as indicated in *Figure: 3-4a.* Increasing the external load further results in full plastic deformation of the cross section, the point at which a further increase of the bending moment resistance is not possible and a failure mechanism is said to have formed (*Figure 3-2*: point B). The bending moment resistance at point A to B in *Figure: 3-2* is visualized by *Figure: 3-3*, where the elastic and plastic bending moment distribution is given through the cross-sectional area of a I-beam.

For statically indeterminate structures like plate models, an increase of the load beyond point B forms a failure mechanism through redistribution of moments. This way the bilinear relation between deformation and stress is lost, *Figure: 3-4b.* Additionally, membrane forces could be considered as part of the resistance curve, *Figure: 3-4c.* Membrane stresses in the plate occur when neighboring structural elements create a strengthening effect during plastic collapse. Since it is assumed the boundary conditions for both plate types are similar and therefore the strengthing created by both boundaries is equal, the additional membrane strength due to the plates being anchored into their adjacent structures is neglected. Through the assumption of a determinate resistance curve, use of the upper bound theorem for yield failure is acceptable and an analytical solution can be obtained.

With the proviso that the effective width is taken into account for elastic deformations, a determinate failure mechanism is generally accepted for stiffened steel plates subjected to a partial load, as only a few stiffeners are affected [15]. Verification of a correctly chosen effective

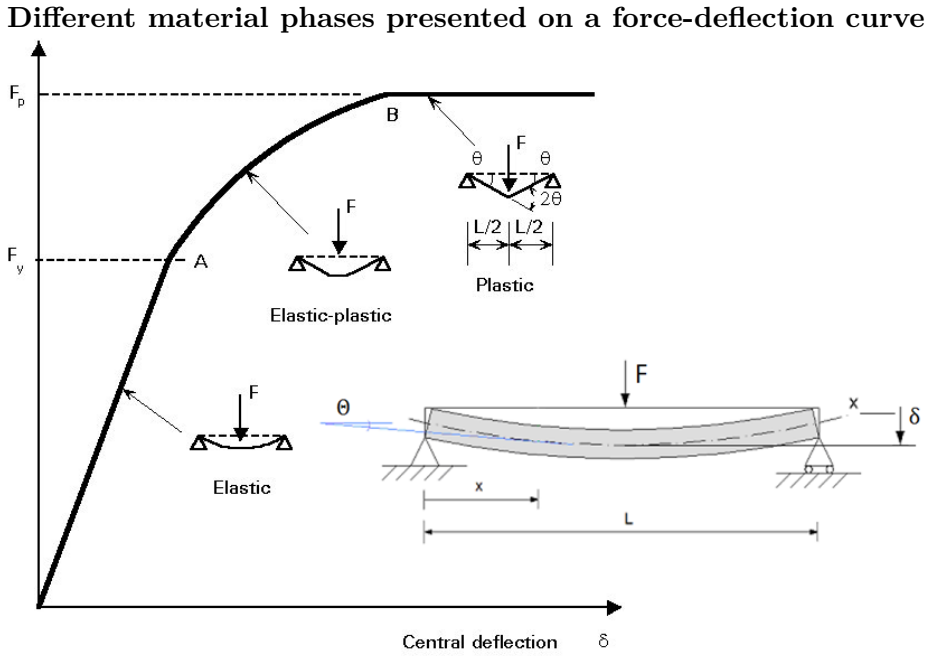

Figure 3-2: A force-deflection curve associated with a simply supported beam failure mechanism (single hinge) for the plastic bending of structures

width for SSP is done by setting up a single hinge simply supported failure mechanism for numerical models with different stiffener distance intervals.

The failure mechanism of a beam is defined by its length and boundary conditions. For a simply supported beam (*Figure: 3-2*) with length L, a plastic hinge forms at its center, resulting in a failure load as presented in *Equation: 3-3*.

$$F \cdot \delta = 2 \cdot \Theta \cdot M_b \tag{3-3}$$

With the assumption of small angular rotations, the angle of rotation Θ is equal to $\frac{\delta}{L/2}$. Hence, the angle of rotation at the beam's center is $2 \cdot \Theta = 4 \cdot \frac{\delta}{L}$. A failure mechanism formula for beam shaped cross-sections is found; *Equation: 3-4*.

$$F = \frac{4}{L} \cdot M_b \tag{3-4}$$

3-2-4 Plate structural geometry

In order to make a comparison between the SSP and SPS structures, the dimensions of the stiffened steel plate reference structure are used. Data on the dropped object area, the geometry of the plate and the effective width are therefore required.

Figure 3-5a provides an overview of the studied dropped object area. Laydown Area 7 is indicated by the red rectangle, for which a single deck plate is considered. The length of the stiffeners, which are not indicated in this figure, are defined by the span of the deck

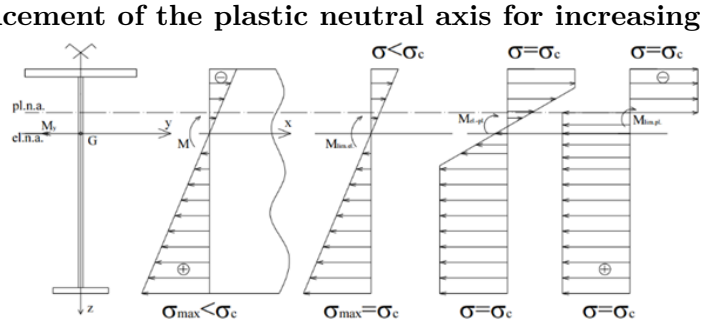

Figure 3-3: Elastic and plastic bending moments through the cross-section of an I-beam

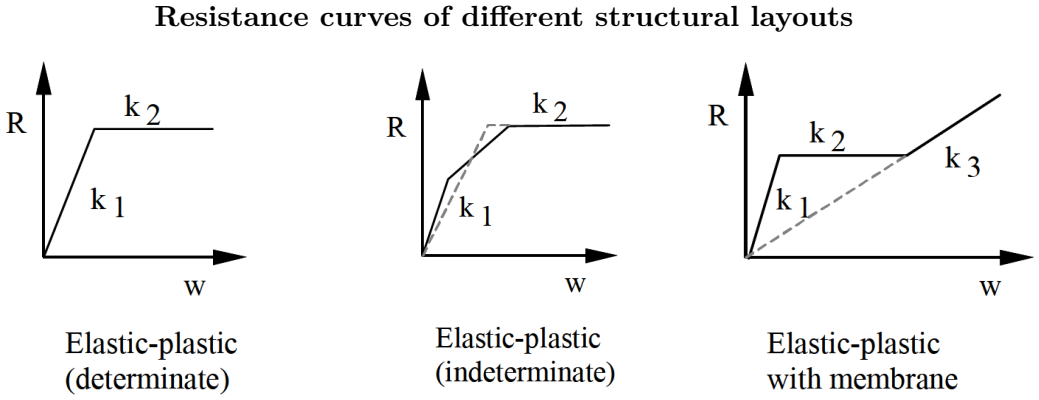

(a) Elastic-plastic determinate resistance curve **(b)** Elastic-plastic indeterminate resistance curve **(c)** Elastic-plastic indeterminate resistance curve with membrane

Figure 3-4: Determinate and indeterminate resistance curves for elastic-plastic materials

plate, $L = 2,875[m]$. The distance between each stiffener is based on preliminary design; $S = 600[mm]$. *Figure 3-5b* provides a cross-section of said stiffeners.

Since only the flange of the SSP structure is considered connected at the boundaries, a reduction in effective width between the stiffeners should be accounted for. A reduction of the effective width due to buckling is neglected for this analysis as the flange of the stiffened steel plate is on the tension side during loading. However, a reduction in the form of shear lag due to an uneven stress distribution is transitioned based on *Figure 3-6*. The effective width factor accounts for the longitudinal shear causing a non-uniform normal stress distribution through the width of the plate during bending. The effective width factor is a function of the distance between stiffeners [S], the length of the stiffeners themselves [L] and boundary conditions of the plate. An effective width of $S_e = 0,7 \cdot S = 420[mm]$ for the stiffeners has been considered.

3-3 Stiffened steel plate yielding

For the stiffened steel plate the elastic- and plastic-bending moment formula are determined providing an indication of the expected internal bending moment resistance. The bending

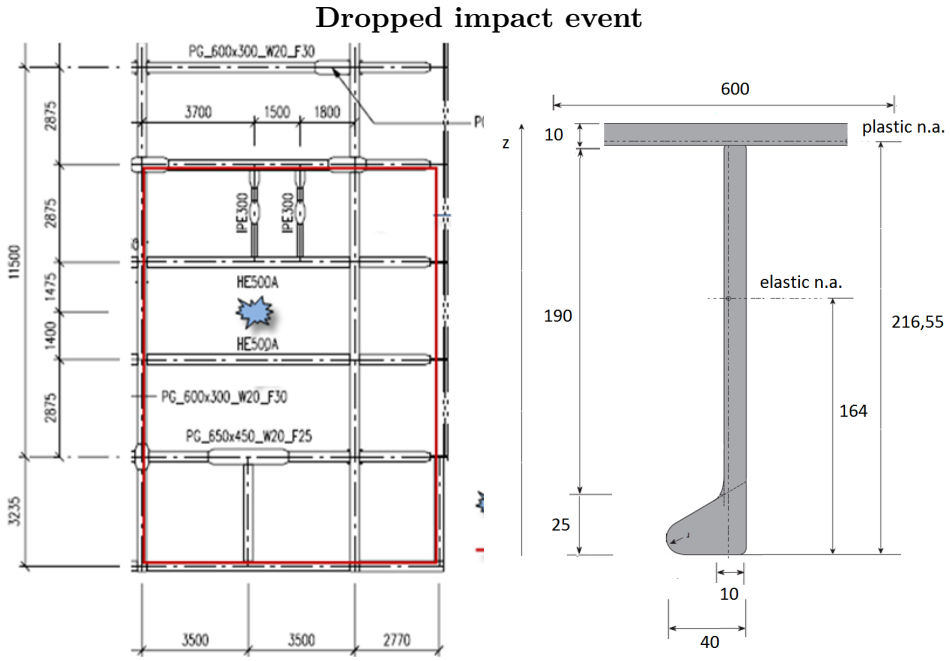

(a) Dropped object scenario at laydown area #7

(b) Cross sectional area of stiffener

Figure 3-5: Stiffened Steel Plate dropped impact scenario

moment resistance of the stiffened steel plate is determined per individual stiffener, where for the elastic bending moment the effective width is taken into account. The yield length is considered by taking into account the total amount of stiffeners 'n' affected by yielding; *Equation 3-5*.

$$M_{SSP} = n \cdot M_{stiffener} \tag{3-5}$$

A shape factor of $\frac{4{,}02}{2{,}78} = 1{,}45$ is found for the SSP-600 structure. This value, which is usually expected for rectangular cross-sections, is explained by the reduction in elastic section modulus due to the effective width factor. During plastic deformations the entirety of the cross-section experience a similar yield stress distribution explaining why the effective width factor is not applicable to the plastic section modulus.

3-3-1 Elastic bending moment SSP

The elastic bending moment per stiffener at maximum elastic deflection of the stiffened steel plate is determined in accordance to *Equation: 3-6*;

$$M_{e,stiffener} = W_{e,stiffener} \cdot \sigma_y, \qquad with; \quad W_e = \frac{I_{stiffener}}{y_{e.n.a.}} \tag{3-6}$$

$$I_{stiffener} = \sum_{1}^{i} I_i + A_i \cdot d_i^2 = I_{plate} + A_{plate} \cdot d_{plate}^2 + I_{web} + A_{web} \cdot d_{web}^2 + I_{bulb} + A_{bulb} \cdot d_{bulb}^2 \tag{3-7}$$

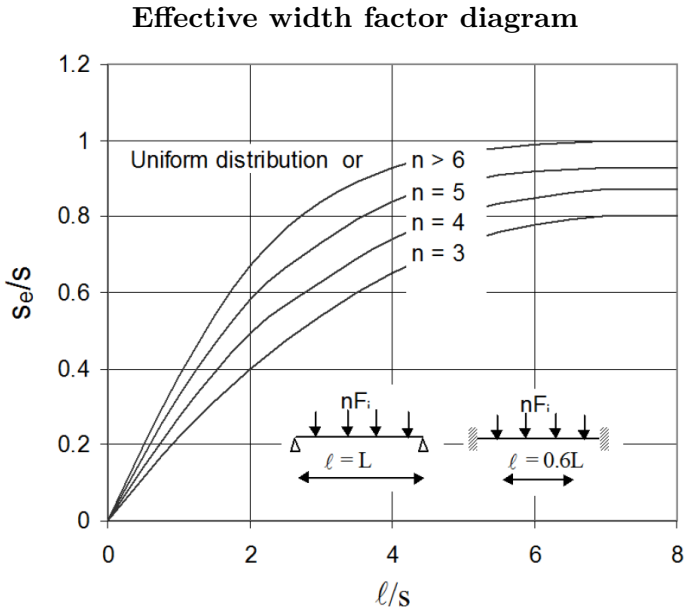

Figure 3-6: The effective width factor for stiffened steel plates

Where;

$$I_i = \frac{1}{12} \cdot b_i \cdot h_i^3 \qquad A_i = b_i \cdot h_i \qquad d_i = y_{e.n.a.} - z_{i,c.o.g.} \tag{3-8}$$

With an elastic neutral axis at 164 mm from the bottom of the bulb, an elastic section modulus of $W_{e,stiffener} = 2,78 \cdot 10^5\ mm^3$ per stiffener (per 600 mm) is found.

3-3-2 Plastic bending moment SSP

The plastic bending moment of the stiffened steel plate per stiffener is determined in accordance to *Equation: 3-9*;

$$M_{p,stiffener} = W_{p,stiffener} \cdot \sigma_y, \qquad with; \quad W_p = \frac{1}{\sigma_y} \cdot (M_{top} + M_{bot}) \tag{3-9}$$

Where M_{top} and M_{bot} are the full plastic bending moments above and below the plastic neutral axis respectively. With a plastic neutral axis at $216,55\ mm$ from the bottom of the bulb, a plastic section modulus of $W_{p,SSP} = 4,02 \cdot 10^5\ mm^3$ is found.

3-4 Sandwich Plate System yielding

The SPS panel's elastic and plastic bending moments are determined for a range of design parameters, as a function of the variables t_{fp}; the face plate thickness, and t_c; the core thickness. Since the panel does vary in thickness over the width of the structure, the elastic- and plastic- bending moments are determined per unit length (width).

3-4-1 Elastic bending moment SPS

The internal bending moments for the sandwich panel are calculated in a similar fashion as the stiffened steel plate. Due to symmetry of SPS, the elastic- and plastic neutral axis are both at the middle of the cross section. The transformation method for composite structures is used, which effectively presumes the SPS cross-section as an I-shaped cross sectional area, where the polyurethane core is reduced to a proportional width. In this case the resulting 'web' is neglectable given the polyurethane material properties.

$$M_{e,SPS} = W_{e,SPS} \cdot \sigma_y \qquad with; \quad W_{e,SPS} = \frac{I_{SPS}}{t_{fp} + \frac{t_c}{2}} \tag{3-10}$$

With the polyurethane core 'web' neglected and assuming that the Kirchhoff plate bending theory is applicable, symmetry gives;

$$I_{SPS} = 2 \cdot I_{flange} + I_{web} \approx 2 \cdot I_{flange} = 2 \cdot (I_{flange} + A_{flange} \cdot d^2_{flange}) \tag{3-11}$$

When I_{SPS} is expressed per unit width b;

$$I_{SPS} \cdot \frac{1}{b_{SPS}} = 2 \cdot (\frac{1}{12} \cdot t^3_{fp} + t_{fp}(\frac{t_{fp}}{2} + \frac{t_c}{2})^2) = 2 \cdot (\frac{1}{3} \cdot t^3_{fp} + \frac{1}{2} \cdot t^2_{fp} \cdot t_{core} + \frac{1}{4} \cdot t_{fp} \cdot t^2_{core}) \tag{3-12}$$

The elastic section modulus for SPS, $W_{e,SPS}$ $[m^3/m]$ (section modulus per unit width), becomes;

$$W_{e,SPS} \cdot \frac{1}{b_{SPS}} = \frac{2 \cdot (\frac{1}{3} \cdot t^3_{fp} + \frac{1}{2} \cdot t^2_{fp} \cdot t_{core} + \frac{1}{4} \cdot t_{fp} \cdot t^2_{core})}{t_{fp} + \frac{t_c}{2}} \tag{3-13}$$

The elastic section moduli for various SPS configurations have been provided in a contour plot; *Figure: 3-7.*

3-4-2 Plastic bending moment SPS

The plastic bending moment for the SPS panel is determined in a similar fashion as the elastic bending moment. However, the strength gained from the core material, which is less than 1% of the total plastic bending moment, has been neglected for the purpose of simplicity.

$$M_{p,SPS} = W_{p,SPS} \cdot \sigma_y, \qquad with; \quad W_{p,SPS} = 2 \cdot t_{fp} \cdot \frac{t_{fp} + t_{core}}{2} \cdot b_{SPS} \tag{3-14}$$

The plastic section modulus (per unit width) formula for SPS, $W_{p,SPS}$ $[m^3/m]$, becomes;

$$W_{p,SPS} \cdot \frac{1}{b_{SPS}} = 2 \cdot t_{fp} \cdot \frac{t_{fp} + t_{core}}{2} \tag{3-15}$$

The plastic section moduli for various SPS configurations have been provided in a contour plot; *Figure: 3-8.*

From both the elastic and plastic contour plots several section moduli of common thickness configurations are provided in *Table: 3-1.* From the shape factors one finds that, at least for

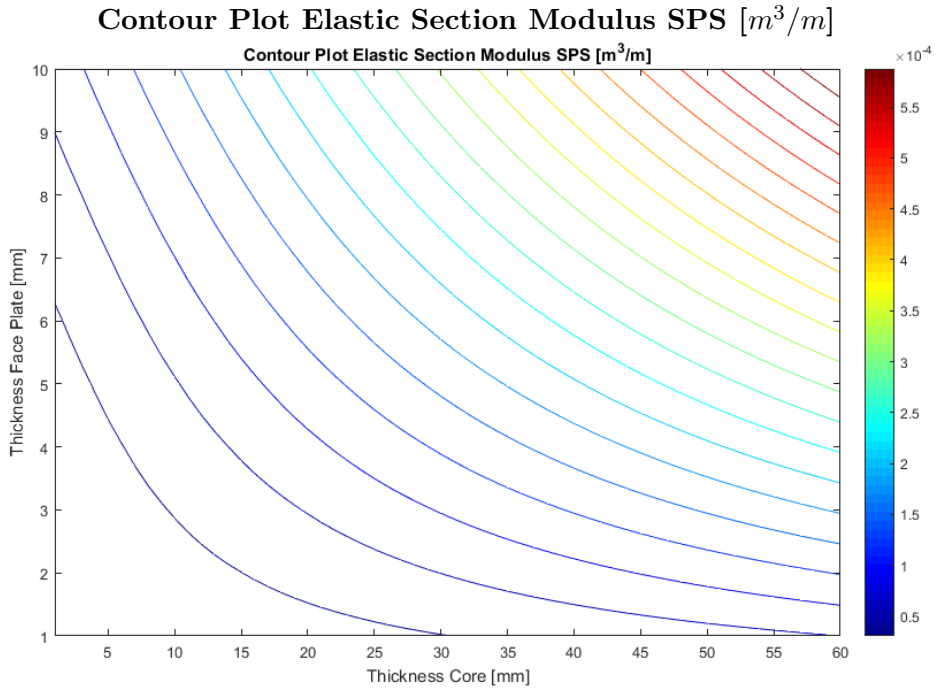

Figure 3-7: A contour plot of the elastic section moduli for various SPS configurations

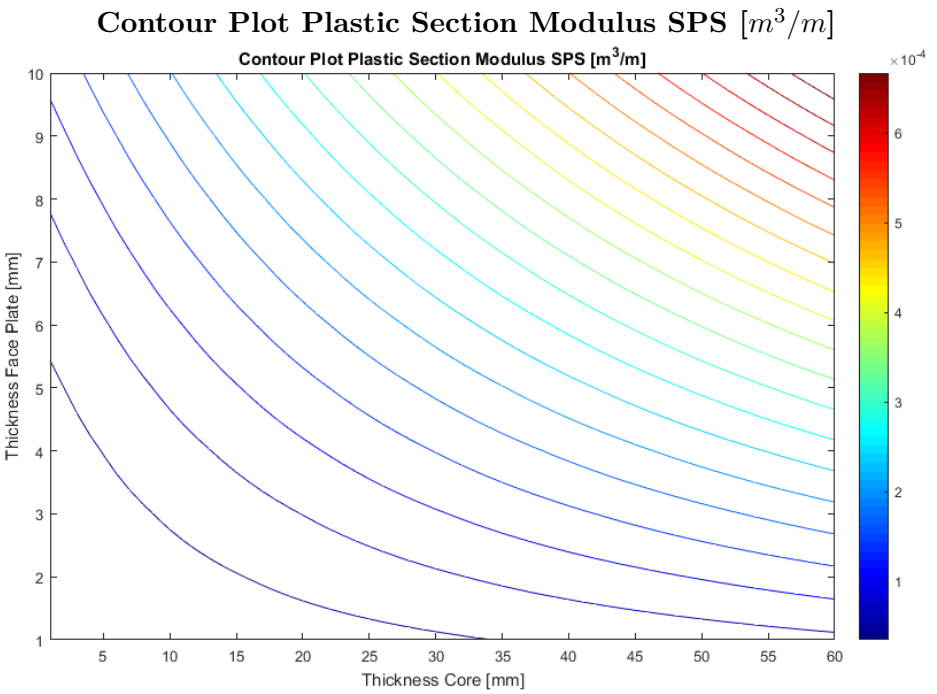

Figure 3-8: A contour plot of the plastic section moduli for various SPS configurations

the assumption of simply supported beam failure, the ductile design assumption might not representative for some of the design thickness configurations. The configurations for which the shape factor is lower than 1,1 the ultimate failure load is expected to exceed the yield

failure load by less than 10% and the ductile design criteria are not met.

The elastic and plastic section moduli of SPS configurations are compared with the section moduli of the SSP reference structure in *Table: 3-2*. Here the section moduli are indicated per stiffener interval distance of 600 mm for most comparable results.

Section Moduli SPS per unit length

Plate	Elastic Section Modulus $[m^3/m]$	Plastic Section Modulus $[m^3/m]$	Shape factor
SPS 3-15-3	$4,67 \cdot 10^{-5}$	$5,40 \cdot 10^{-5}$	1,16
SPS 3-30-3	$9,10 \cdot 10^{-5}$	$9,90 \cdot 10^{-5}$	1,09
SPS 3-45-3	$1,36 \cdot 10^{-4}$	$1,44 \cdot 10^{-4}$	1,06
SPS 5-15-5	$8,17 \cdot 10^{-5}$	$1,00 \cdot 10^{-4}$	1,22
SPS 5-30-5	$1,54 \cdot 10^{-4}$	$1,75 \cdot 10^{-4}$	1,13
SPS 5-45-5	$2,28 \cdot 10^{-4}$	$2,50 \cdot 10^{-4}$	1,10
SPS 5-60-5	$3,02 \cdot 10^{-4}$	$3,25 \cdot 10^{-4}$	1,08
SPS 10-30-10	$3,27 \cdot 10^{-4}$	$4,00 \cdot 10^{-4}$	1,22
SPS 10-45-10	$4,71 \cdot 10^{-4}$	$5,50 \cdot 10^{-4}$	1,17

Table 3-1: The elastic and plastic section moduli per meter of common SPS thickness configurations

Section Moduli SPS per 600 $[mm]$

Plate	Elastic Section Modulus $[m^3/m]$	Plastic Section Modulus $[m^3/m]$
SPS 3-15-3	$2,80 \cdot 10^{-5}$	$3,24 \cdot 10^{-5}$
SPS 3-30-3	$5,46 \cdot 10^{-5}$	$5,94 \cdot 10^{-5}$
SPS 3-45-3	$8,16 \cdot 10^{-5}$	$8,64 \cdot 10^{-5}$
SPS 5-15-5	$4,90 \cdot 10^{-5}$	$6,00 \cdot 10^{-5}$
SPS 5-30-5	$9,24 \cdot 10^{-5}$	$1,05 \cdot 10^{-4}$
SPS 5-45-5	$1,37 \cdot 10^{-4}$	$1,50 \cdot 10^{-4}$
SPS 5-60-5	$1,81 \cdot 10^{-4}$	$1,95 \cdot 10^{-4}$
SPS 10-30-10	$1,96 \cdot 10^{-4}$	$2,40 \cdot 10^{-4}$
SPS 10-45-10	$2,826 \cdot 10^{-4}$	$3,30 \cdot 10^{-4}$
SSP 600	$2,78 \cdot 10^{-4}$	$4,02 \cdot 10^{-4}$

Table 3-2: The elastic and plastic section moduli per 600 mm length of SSP and common SPS thickness configurations

3-5 SPS preliminary design parameters

A large variation of design possibilities is available for SPS panels. To find realistic design configurations for the SPS panel, initial design limitations are set.

- Limitation 1: Mass of SPS per area < Mass SSP per area
- Limitation 2: Minimum thickness requirement SPS; $t_{fp} \geq 3$ [mm], $t_c \geq 15$ [mm]

The first limitation is set to ensure SPS is financially more viable than SSP. Although installation and fabrication costs of SPS may exceed those of SSP, the assumption where lower weight equals lower overall costs is used as a starting point. The second limitation is set to produce reliable, high quality SPS panels with a minimum thickness of the face plate and core, required to get insurance of offshore facility insurer companies.

A comparison is made between the mass of the stiffened steel plate and various SPS configurations. The mass difference ratio μ, has been determined for both plate type structures per square meter, *Equation: 3-16*.

$$m_{SPS} \cdot \mu = m_{SSP} \tag{3-16}$$

The mass of SPS (m_{SPS}) and SSP (m_{SSP}) are determined with the following equations respectively; *Equation: 3-17 & 3-18*.

$$m_{SPS} = (2 \cdot t_{tp} \cdot \rho_{S355} + t_{core} \cdot \rho_{PU}) \tag{3-17}$$

$$m_{SSP} = (t_{flange} + (t_{bulb} \cdot w_{bulb} + t_{web} \cdot w_{web}) \cdot n_{spm}) \cdot \rho_{S355} \tag{3-18}$$

Where in *Equation: 3-18* the ratio $n_{spm} = 0,77$ indicates the amount of stiffeners per meter for SSP-600.

By substitution of *Equation: 3-17* and *Equation: 3-18* into *Equation: 3-16*, one finds the difference factor in mass of SPS compared to SSP, graphically presented in *Figure: 3-9*. Here, for $\mu \geq 1$, the mass of the SPS thickness configurations are lower than the stiffened steel plate. The thickness configurations of the area below the black line drawn in *Figure: 3-9* indicates which designs have a lower mass than SSP-600. One finds the amount of possible SPS designs having a mass lower than SSP-600 is limited to a maximum face plate thickness of 5 mm at a core thickness of 15 mm or maximum a core thickness of 45 mm at a face plate thickness of 3 mm.

Similar to the mass contour plot, a contour plot is made for the elastic and plastic section moduli are provided in *Figure: 3-10* and *Figure: 3-11*. Here the area below the black line indicates the configurations for which the mass is lower for SPS compared to SSP. It can be noted that for no thickness configurations an increase in elastic or plastic bending moment is found. Thus, the SPS configurations for which the bending resistances are higher, the mass of the configurations is also higher.

3-6 Preliminary conclusion

Based on this preliminary analytical study, it can be concluded that the dropped object impact is likely governed by boundary controlled plate response, for which quasi-static loading may be considered.

When yielding due to pure bending is considered, taking into account bilinear materials and a mass limit, SSP offers a better resistance to quasi-static loading. However, since the energy

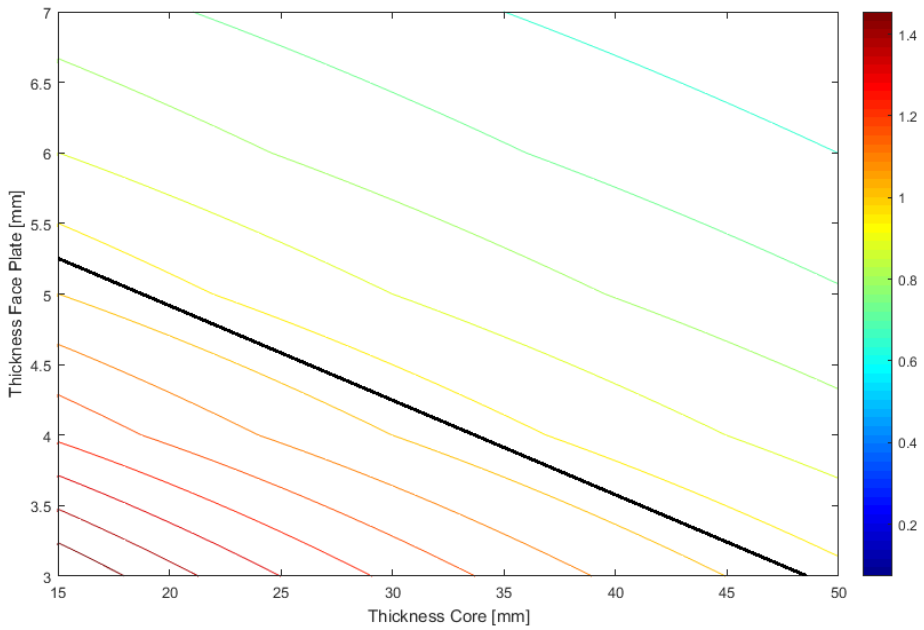

Figure 3-9: The weight reduction of SPS configurations compared to the SSP reference structure

dissipated before failure by both structures is determined not only on loads but also by deflection, one should take into account the maximum deflection before failure.

Due to the difference in thickness, the deflection limit for SSP and SPS are different. SPS starts deforming plastically for a further deflection level, one at which the ductility ratio as chosen for SSP is likely a non-acceptable limit. This translates into a greater dissipated energy before failure.

Thus, although the bending moment resistance of SSP exceeds SPS for an equivalent mass, the additional deflection SPS can undergo before failure may lead to a relatively greater dissipated energy.

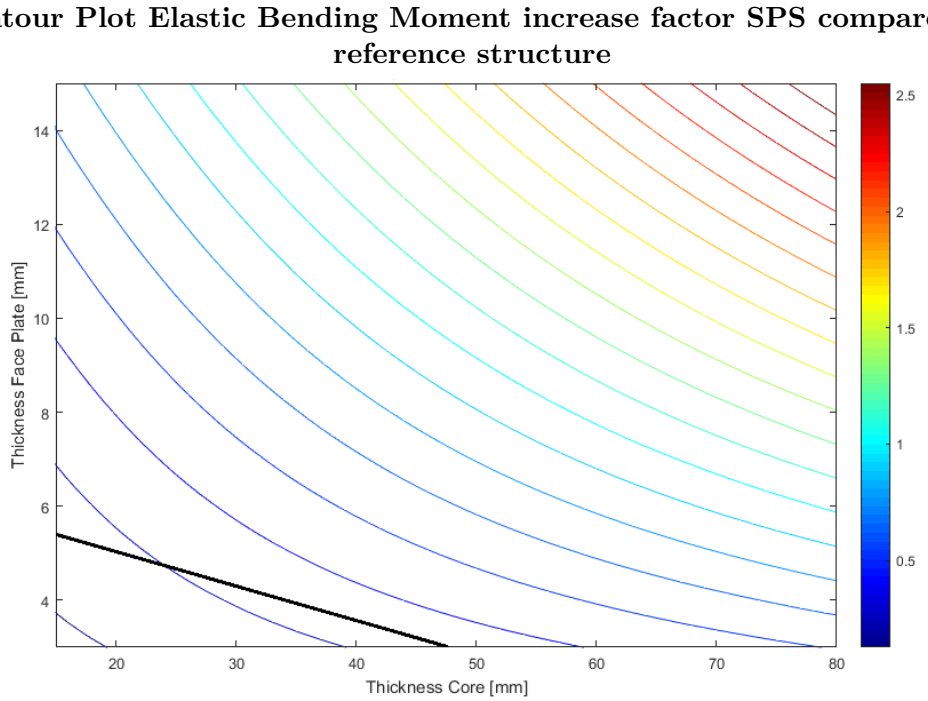

Figure 3-10: The difference in Elastic Bending Moment between SSP and a range of SPS thickness configurations

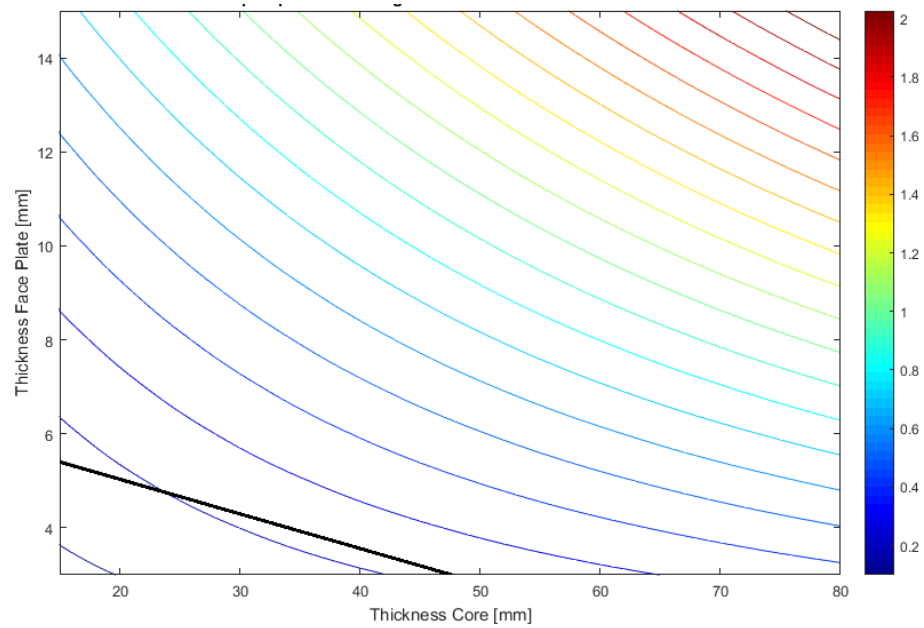

Figure 3-11: The difference in Plastic Bending Moment between SSP and a range of SPS thickness configurations

Chapter 4

Finite Element Modeling

In order to simulate impact behaviour, various structural analysis software is available. In this research the ANSYS APDL software package for structural analyses has been used with an Academic Teaching license. ANSYS APDL focuses on analyses of single unit structures. The software lends itself for modeling of basic areas and volumes using direct generation, which offers the shortest way to generate finite element meshes. The use of scripts makes ANSYS APDL a flexible and suitable software package for multi-case analyses.

Scripts for multiple models and analysis controls (load applications) have been drafted in the form of text files for both SSP and SPS beam- and plate- structures. The beam models have been used for verification of the analytical study, while the plate structures were used for finding an optimal solution to impact loads from dropped object structures.

4-1 Mathematical Model

When the dynamic impact of a dropped object is treated as a quasi-static load as described in *Chapter: 3*, the structural analysis for static solutions can be used to describe the plates impact response. The static analysis solution method in ANSYS uses Newton's second law, where inertial- and damping effects are ignored; *Equation: 4-1*.

$$[K]\{u\} = \{F\} \tag{4-1}$$

Here $[K] = \sum_0^n [K_e]$, with $[K_e]$ the element stiffness matrix and n the number of elements.

The stiffness matrix $[K]$ is determined from the finite element discretization process which yields a set of simultaneous equations for each element. For plastic deformations $[K]$ is a function of the unknown degree of freedom values, making it a non-linear equation. To solve this non-linear equation, the use of an iteration method is required. For path-dependent nonlinearities such as plasticity the solution process requires that some intermediate steps are in equilibrium in order to correctly follow the load-deformation path. This requirement has been fulfilled by specifying a step-by-step incremental analysis using the Incremental Newton-Raphson Procedure, otherwise known as the full Newton-Raphson solution procedure.

4-2 Finite Element Model

A total of five different models have been considered, 2 in the form of SSP and 3 in the form of SPS. The cases have been distinguished based on their geometric sizes, where beam- and plate models are used for verification and results on the research question respectively.

4-2-1 Boundary Conditions

Verification of the yielding failure mode has been conducted by considering pure bending. To do so, simply supported boundary conditions were applied to the verification models, preventing hinges from forming at the boundaries of the structure. The applied boundary conditions for the numerical models have been illustrated in *Figure: 4-1ba*. The shortest opposite edges for the beam model and the whole perimeter for the plate model are fixed in vertical direction (z-axis). Distinction between the two is indicated by round brackets. To prevent in-plane rotation, two corner nodes have been restricted from moving in the horizontal direction (x-axis). The assumption of pure bending for both plate and beam models is realized by restricting a single node from moving in the horizontal (y-axis) direction. Finally, an additional boundary condition has been implemented for the stiffened steel models, where the stiffeners have been restricted from moving horizontally (x-axis) to prevent rotation of said stiffeners around the y-axis; *Figure: 4-1bb*. This restriction has been implemented as a most conservative case, where the stiffeners offer the highest possible stiffness. For loads applied only in vertical direction and not taking into account geometric non-linearities, these boundary conditions have shown to be sufficient and a minimal difference in analytical and numerical output is found.

4-2-2 Applied loads

Three distinct load cases have been analyzed for the considered models in the form of loads and deflections. Graphically represented in *Figure: 4-2ba, Figure: 4-2bb,* and *Figure: 4-3* are the load cases applied on the SSP structure. The load cases for the SPS structure are not presented here, but have been applied in a similar fashion.

The first load case, two point loads on top of the stiffeners at the center of the span, was applied to analyze the difference in results when a load instead of a deflection is considered; *Figure: 4-2ba*. By considering point loads, local deformation effects are eliminated and a single hinge line failure mechanism, similar to the one expected when the structure is subjected to a line deformation, is ensured. The second load case, a line load as presented in *Figure: 4-2bb*, showed minimal differences with the first load case applied, but proved impractical due to the element size dependency. Although the second case seems a more logical choice, it has therefore not been considered in further analyses. The third load case, a circular load, has been applied to represent the dropped object load, *Figure: 4-3*.

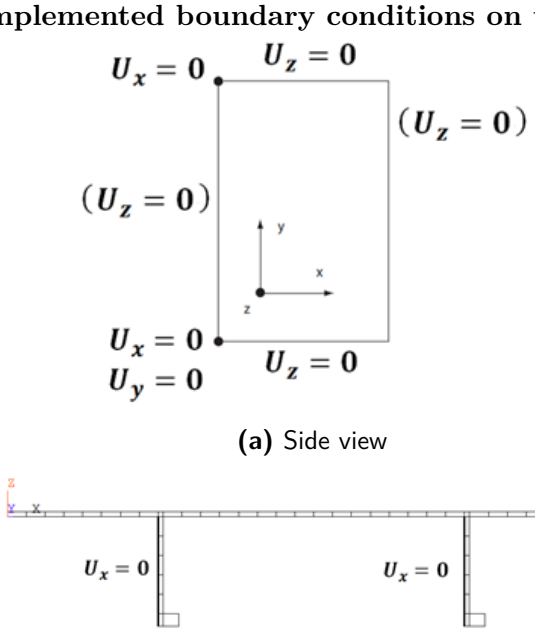

(a) Side view

(b) Top view

Figure 4-1: A top and side view of the numerically applied boundary conditions for the SSP & SPS and SSP structures respectively

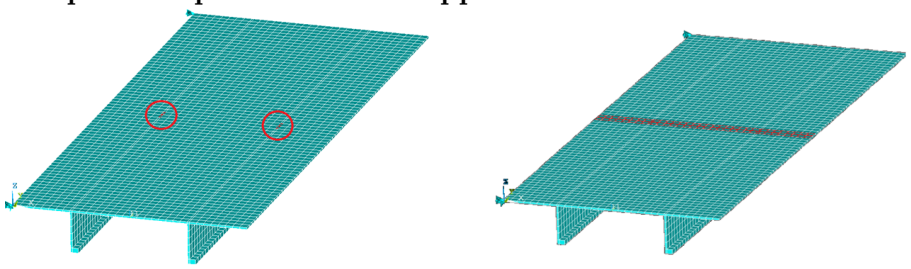

(a) Numerically applied loads SSP-600 model; point loads

(b) Numerically applied loads SSP-600 model; line load

Figure 4-2: SPS and SSP applied load types; Point loads and line loads

4-2-3 Element type & Meshing

Element type

A single element type, SOLID186, has been used for both the SSP and SPS models, *Figure: 4-4*. SOLID186 is a solid, second order element having 20 nodes with each 3 degrees of freedom (x, y and z-direction). This element type offers the ability to model very local bending effects, while it prevents shear locking and hourglassing through its quadratic element property.

Shear locking is an effect which occurs for materials under pure bending. Elements subjected to pure bending ideally experience a curved shape change, of which linear elements are unable. For linear elements shear locking introduces an incorrect artificial shear stress, which

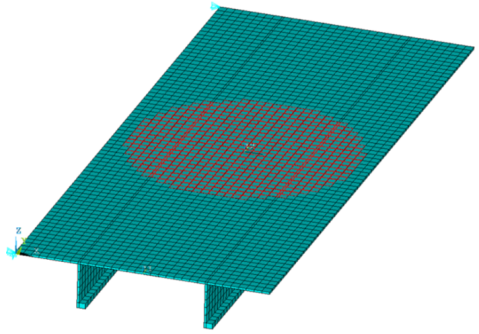

Figure 4-3: SPS and SSP applied load types; circular load

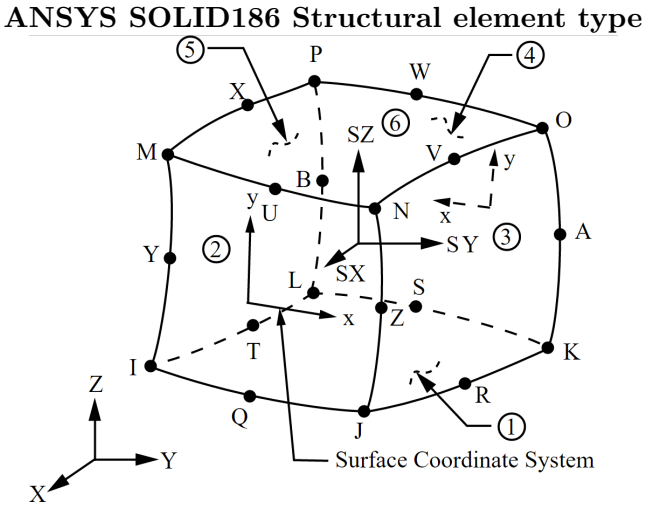

Figure 4-4: ANSYS second order element type having 20 nodes with each 3 degrees of freedom; SOLID186

means the strain energy in the element is generating shear deformation instead of bending deformation. The overall effect is that linear fully integrated elements become locked or overly stiff under the bending moment. Quadratic elements do not experience shear locking due to the introduction of additional nodes.

The decrease in computational efficiency, which the additional nodes bring as an undesirable effect, has been minimized by using a reduced integration solution. A side effect of reduced integration is that it may result in excessively flexible elements, also known as the hourglassing effect. When hourglassing occurs meaningless results are produced as the single integration point over the element's sides assume normal stresses and shear stresses to be zero at the point of integration. Second order solid elements may suffer from hourglassing when a single layer of elements is used through the thickness of the panel. For the models used in this study, hourglassing has been prevented by using multiple elements through the thickness where possible or by using full integration when mesh densities were to result in shape limit warnings.

Meshing

Based on the element convergence study conducted in *Appendix: C*, mesh densities have been chosen for the SSP and SPS models. For both models the elements have a proportional spacial discretization of 8 *mm* along the length and width of the structure. Through the thickness of the SPS panel a minimum of 5 elements have been considered, where the faceplates consist of a single element, while the core has three. *Table: 4-1* provides an overview of the mesh densities for the used models, graphically presented in *Figure: 4-5*.

Thickness [mm]	Element size [mm]	Element layout [L*W*T]	Amount of elements
SSP 600 (1200x2875)	80	36*(18*1+2*5)	1008
SSP 600 (7200x2875)	80	6*(36*(18*1+2*5))	6048
SPS 5-15-5 (50x2875)	40	72*2*5	720
SPS 5-15-5 (1200x2875)	80	36*16*5	2880
SPS 5-15-5 (7200x2875)	80	6*(36*16*5)	17280

Table 4-1: Mesh element distribution for the SSP & SPS models

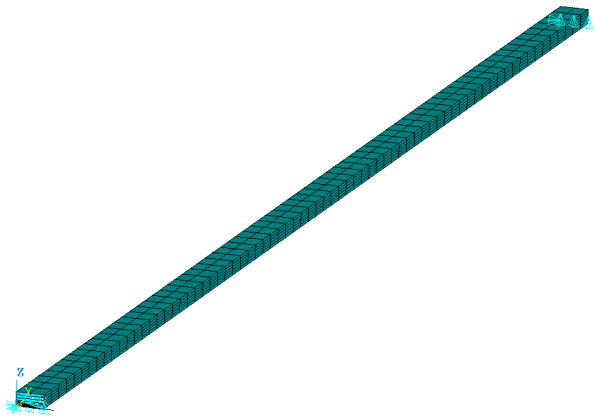

(a) SPS 5-15-5 (50x2875)

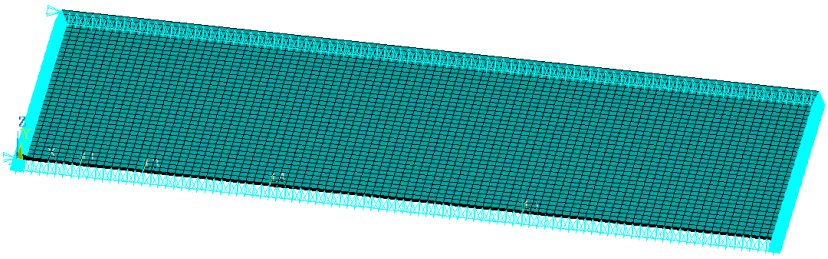

(b) SPS 5-15-5 (7200x2875)

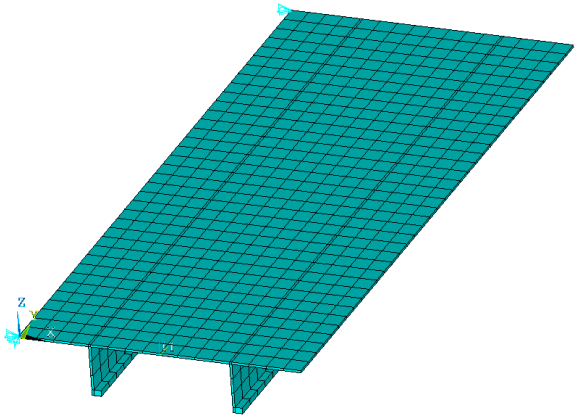

(c) SSP-600 (1200x2875)

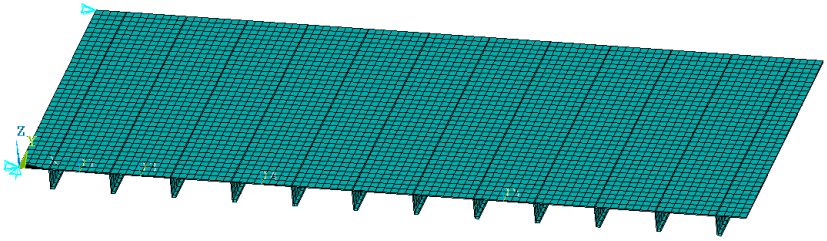

(d) SSP-600 (7200x2875)

Figure 4-5: The Finite Element Models for SSP and SPS

Chapter 5

ANSYS Finite Element Analysis

The preliminary conclusions drawn from the analytical study indicated any thickness configurations for SPS panels (with a mass lower than the SSP panel) to have a lower stiffness and failure load. Despite a certain minimum stiffness to be retained in order to prevent excessive deflection during static loading, the total dissipated energy of these SPS panels against impact loads could potentially be higher due to the greater deceleration distance before failure.

In this chapter the numerical results of quasi-static analyses for SSP-600 and multiple SPS panel configurations subjected to circular deflections are described. An optimal SPS configuration has been sought for by separating the discussed results into four sections; simply supported beam models SSP600 and SPS (1200x2875) and simply supported plate models SSP-600 and SPS (7200x2875).

Comparisons between the SSP-600 panel and the various SPS configurations have been made for governing failure mechanisms, force-deflection curves and dissipated energy diagrams. Based on these results conclusions have been drawn regarding;

- The unaccounted for effects when the assumption of a beam- instead fo a plate model is made
- The deformations of the structures when subjected to a circular load in contrast to line loads
- The stiffness of the structures and their viability as dropped object impact protection

Finally, the range of the impact duration for which the quasi-static load assumption is acceptable has been determined. Based on these results the panel configurations which require further research in the form of a numerical transient solution have been selected.

5-1 Simply Supported Beam Structures (1200x2875)

5-1-1 Failure mechanisms for simply supported beams (1200x2875) subjected to a circular load

To determine whether the found failure load of the structure is plausible, the failure mechanism associated with the structure and its applied load has been considered. Shown in *Figure: 5-1*, the circular deflection applied to the SSP beam structure leads to plastic deformation near the perimeter of the deflection, indicating a circular failure mechanism with two hinge lines is governing. The made analytical assumption of a single hinge at the middle of the span is thus not representative for circular impact loads having a large impact radius.

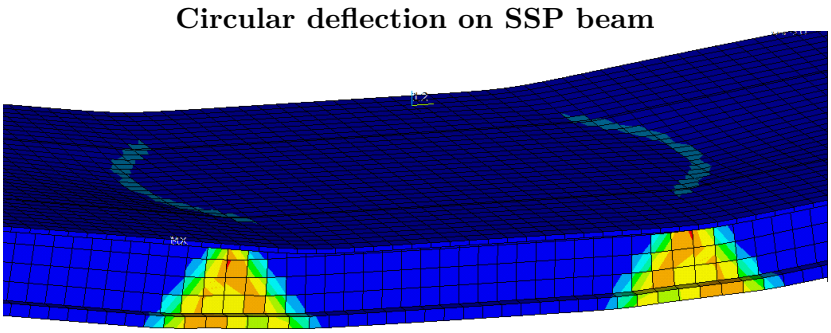

Figure 5-1: Plastic deformations form a double yield line failure mechanism in the SSP-600 structure (1200x2875)

Similar to the stiffened steel beam, the SPS structure develops a failure mechanism with two hinge lines along the perimeter of the applied deflection, see *Figure: 5-2*.

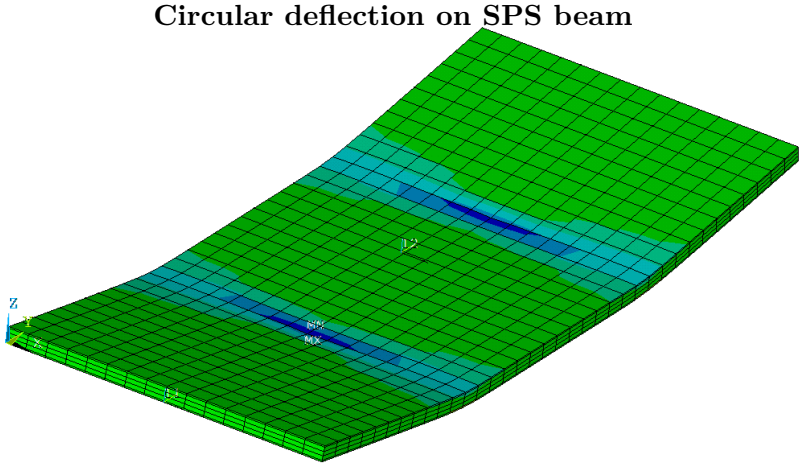

Figure 5-2: Plastic deformations form a double yield line failure mechanism in the SPS 5-45-5 structure (1200x2875)

5-1-2 Force-Deflection Curve and Energy Dissipation for simply supported beams (1200x2875) subjected to a circular load

The force deflection curves for two simply supported beam cases (SSP600 and SPS 5-45-5) subjected to a circular load have been plotted in *Figure: 5-3*. The found failure loads for both models are provided in *Table: 5-1*.

Force-deflection curves SSP-600 and SPS 5-45-5 (1200x2875) when subjected to a circular load

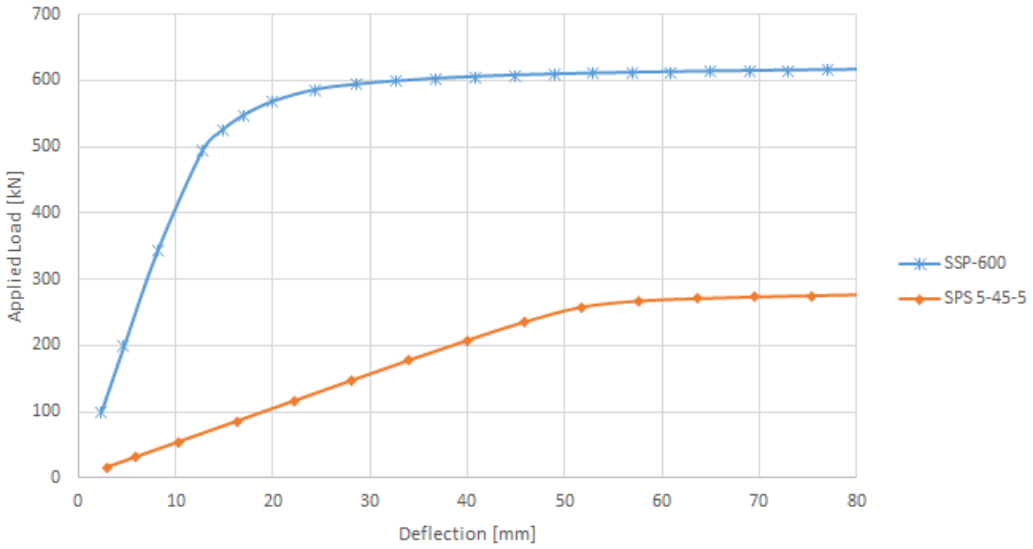

Figure 5-3: The Force-Deflection curve for circular loaded beam models; SPS 5-45-5 & SSP-600 (1200x2875)

Compared to the failure load found for the verification model, for which a singular hinge line failure mechanism was governing, the found governing circular failure mechanism results in a higher failure load for both models. This is explained by the additional length over which yielding occurs. A factor 1,5 difference is found between the two mechanisms, indicating the assumption of a single load point or line often made in analytical calculations is invalid for circular dropped load areas as the bending resistance differs over 50% compared to the analytical result. Additionally, it can be concluded that the difference in failure mechanism does not seem to influence the failure load for different cross-sections of beams. In other words, the shift of failure mechanisms does not seem to affect the optimal choice on beam type structures when the impact load is applied over the full width of the structure.

Plate Structure (1200x2875)	Single Hinge Failure Load [N]	Circular Hinge Failure Load [N]	Difference Factor
SSP 600	402.375	620.000	1,542
SPS 5-45-5	185.916	280.000	1,506
Difference factor	2,16	2,2	-

Table 5-1: A comparison between the failure loads of single and circular hinge failure mechanism of SSP600 and SPS 5-45-5 (1200x2875)

5-2 Simply Supported Plate Structures (7200x2875)

5-2-1 Failure mechanisms for simply supported plates (7200x2875) subjected to a circular load

The SSP600 (7200x2875) panel, subjected to a circular deflection with a diameter slightly larger than the distance between both stiffeners, experiences a failure mechanism where 2 yield lines are formed, similar to the beam model discussed previously; *Figure: 5-4*. Again yielding is initiated in both stiffeners at the bulb, near the perimeter of the applied deflection.

Yielding in the stiffeners of the SSP-600 model

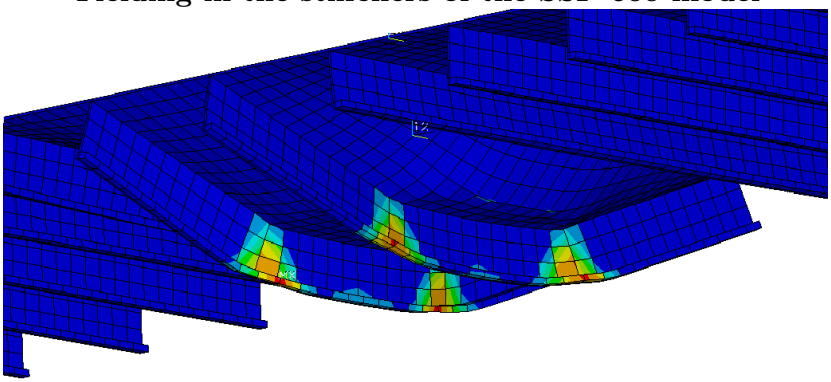

Figure 5-4: Plastic deformations form a circular failure mechanism in the SSP-600 structure (7200x2875)

For the SPS (7200x2875) structure subjected to a circular load, a partially developed circular failure mechanism is found. Similar to the beam structure, plastic yielding is initiated at the perimeter of the applied load closest to the boundaries, see *Figure 5-5*.

Partial circular yield pattern in the SPS 5-45-5 model

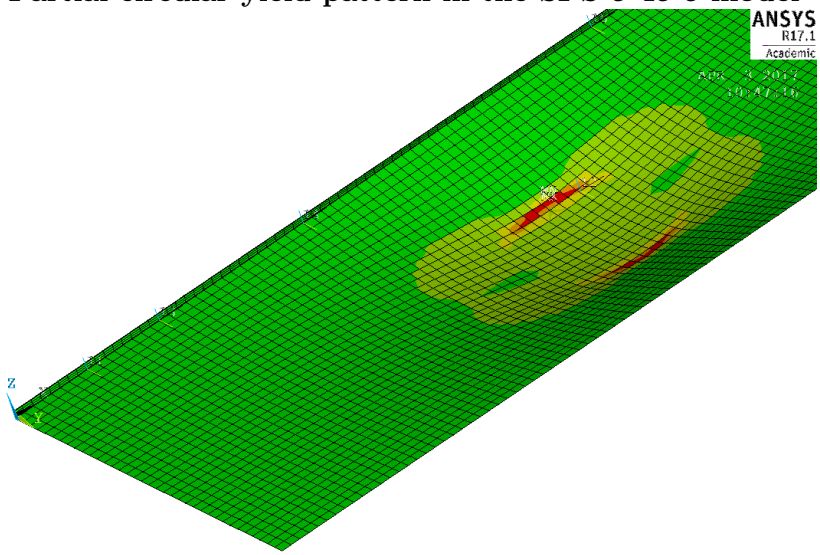

Figure 5-5: Plastic deformations form a partial circular failure mechanism in the SPS 5-45-5 structure (7200x2875)

5-2-2 Force-Deflection Curve and Energy Dissipation for simply supported beams (7200x2875) subjected to a circular load

The force-deflection diagrams associated with the previously mentioned failure mechanisms for the considered plate structures are shown in *Figure 5-6*. Here, the deflection at the middle of the plate is plotted versus the applied external load. Besides the failure load, the figure provides an indication on the stiffness of the structure, as well as the deflection at which plastic deformation is initiated.

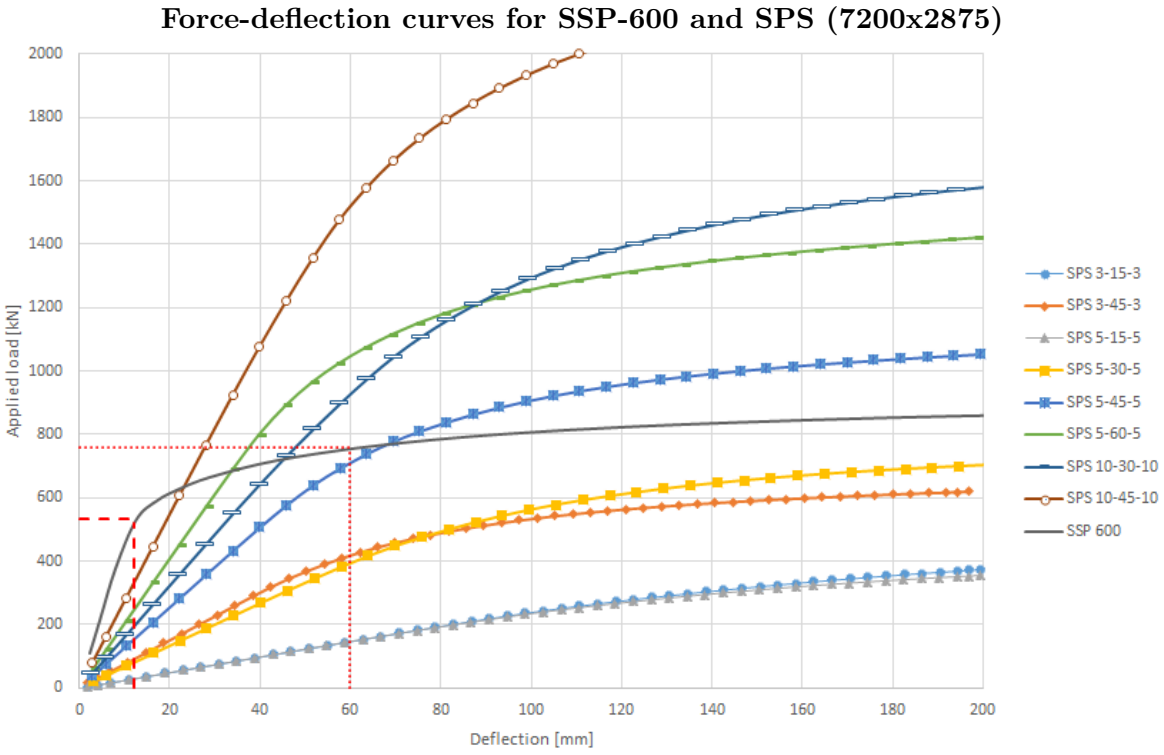

Figure 5-6: Force-deflection curves for plate structures (7200x2875) with different thickness geometries

The deshed and dotted lines in *Figure: 5-6* respectively represent the deformation before elastic and plastic failure of the SSP-600 plate type. For SSP-600 a deflection of 12 mm is found at initiation of plastic deformations using a plastic strain-deflection curve, *Figure: 5-7*. With a ductility ratio $\mu = 5$, a failure deflection of $\delta_{failure} = 60$ mm is found for the SSP case. By extrapolation of the curve, the ultimate strain limit for S355; $\epsilon_u = 0,15$, the maximum deflection for the SSP structure is found at 320 mm. Since the assumption of small angular rotations is valid for deflections up to 375 mm, non-linear geometric effects are not required to be taken into account.

Similarly the elastic and plastic deformation limits are deteremined for the SPS configurations in *Figure: 5-7*, where the plastic strain at the element of first plasticity is plotted versus the deflection at the middle of the plate.

Because of the thinner plate thickness of SPS compared to SSP, the maximum deflection before ultimate strain is reached is larger. Through extrapolation of *Figure: 5-7* it is found that the

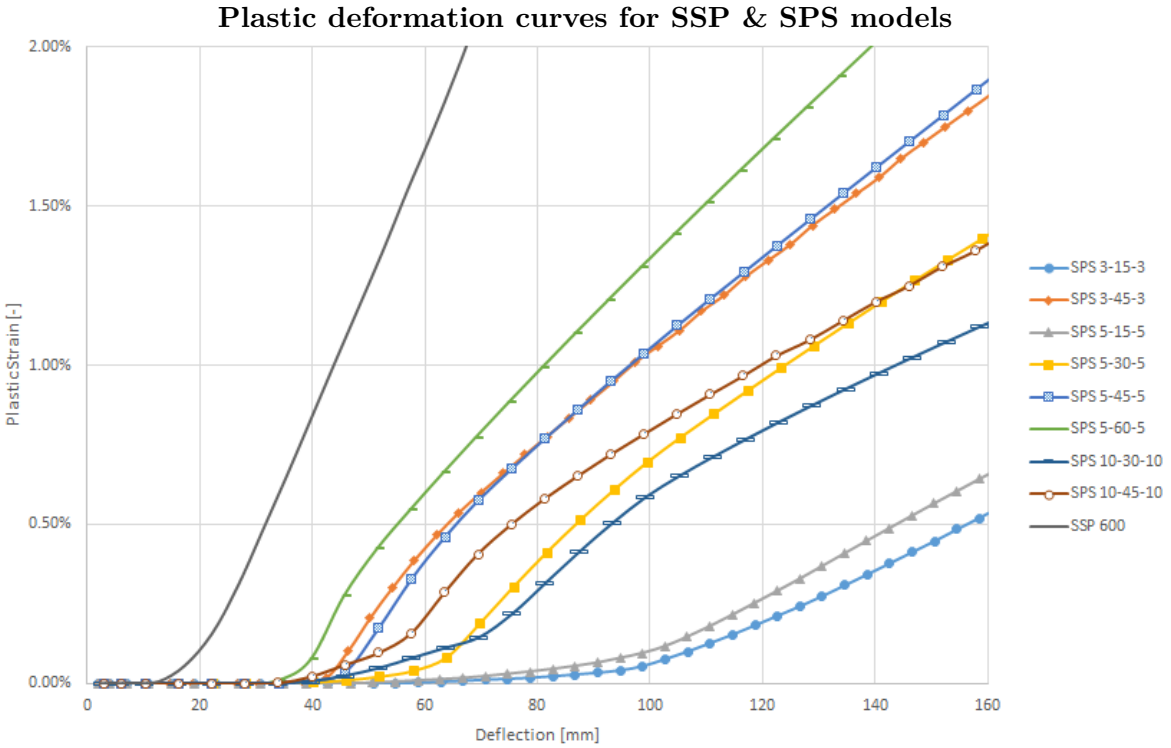

Figure 5-7: Plastic strain at point of first plasticity as a function of the deflection at the impact's center for various plate models (7200x2875)

ultimate deflection limit exceeds 375 mm and thus non-linear effects should be accounted for, as the assumption of small angular rotations is no longer valid. For the thinnest configurations in particular, SPS 3-15-3 and SPS 5-15-5, even a ductility ratio $\mu = 5$ leads to non-linear geometric effects. Since these effects have not been taken into account during the analysis, a deflection limit was set for the SPS configurations based on the deflection limit of the SSP reference structure. Based on the SSP reference structure a maximum angular rotation of 5 degrees was set, *Equation: 5-1*.

$$\delta_{failure} = \frac{2875}{2} \cdot 0,05 = 72mm. \tag{5-1}$$

Remarkable is the additional yield resistance SPS gains from the transverse direction over which yielding takes place compared to the SSP-600 model; *Table: 5-2*. Since the SSP-600 model does not provide stiffness in the transverse direction, the yield failure load increases by only 20% compared to the beam model. The yield resistance of the SPS model on the contrary increases by 190%, resulting in a higher failure load than the SSP-600 model.

Figure 5-8 indicates the maximum dissipated energy for each configuration. When the SPS cases are compared to the SSP reference structure, one finds;

- Configurations SPS 3-15-3 and SPS 5-15-5 are non-viable configurations. Their maximum energy dissipated is less than the SSP-600 panel, while also having a lower stiffness.

Plate Structure (1200x2875)	Beam Structure (1200x2875) Failure Load [N] at 100 [mm]	Plate Structure (7200x2875) Failure Load [N] at 100 [mm]	Difference factor
SSP 600	620.000	750.000	1,21
SPS 5-45-5	280.000	820.000	2,93
Difference factor	2,2	0,91	-

Table 5-2: A comparison between the failure loads of beam and plate configurations SSP600 and SPS 5-45-5

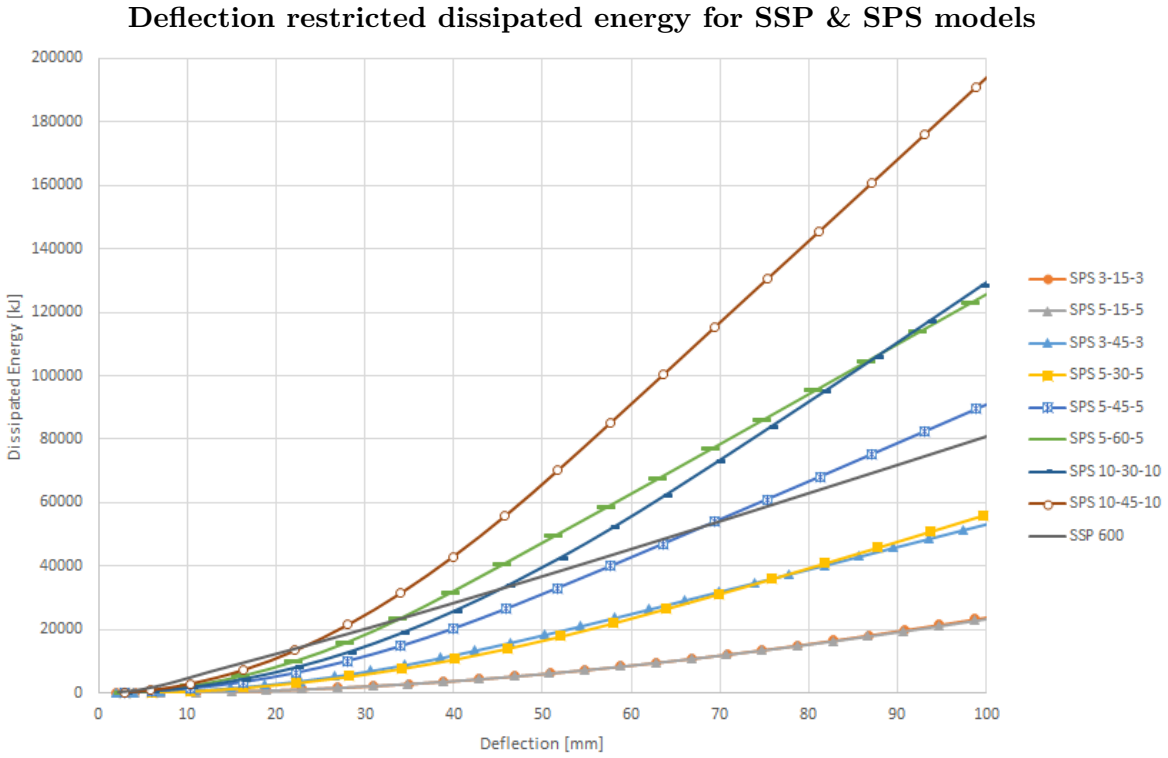

Figure 5-8: Energy dissipated by plate structures as a function of the deflection limited by a maximum value (7200x2875)

- Configurations SPS 3-45-3 and SPS 5-30-5 have a greater total dissipated energy when no limit is set to the maximum deflection. However, when the deflection limits are taken into account, a total dissipated energy lower than the reference structure is found. To consider these configurations as viable options, a greater deflection limit must be accepted.

- The SPS 5-45-5 configuration is able to dissipate energies equal to the SSP-600 model for a center deflection of 60 *mm*. When deflections beyond the limit set for SSP-600 are acceptable, SPS 5-45-5 is superior to SSP-600. However, the stiffness of this configuration remains significantly lower and when subjected to static loads in the elastic deflection range will deform more than twice as much.

- The configurations; SPS 5-60-5 and SPS 10-30-10 have greater dissipated energy levels than SSP-600 before failure is initiated. Although their stiffnesses remain lower, it is a

superior option to SSP-600 when impact loads are considered and neither the mass of the structure or dead loads are important.

- The SPS 10-45-10 configuration exceeds the dissipated energy of SSP-600 significantly. It's stiffness however still does not match that of SSP-600 and it is much heavier per square meter, making this configuration unacceptable

All of the SPS configurations which are able to dissipate more energy than the SSP-600 configuration also have a greater mass per square meter, except for the SPS 3-45-3 and SPS 5-30-5 configuration when deflection limits are not taken into account. For simply supported plate structures (7200x2875) it is thus possible to reduce the mass of the currently used plate structures by using a SPS configuration, but one must take into account the reduced stiffness that comes with it.

The required additional stiffness may be found in the from of clamped boundary conditions. An increase of this stiffness will reduce the deceleration distance, but at the same time increases the total load resistance before failure.

5-3 Range of Dropped Object Impact Durations

Previous research has shown that impact durations of 60 to 200 *ms* are conventional for dropped impact loads of 2000 *kg* on plates with thicknesses and impact velocities similar to the ones considered in this research [2].

The range of dropped object impact durations, for which the researched plate responses are boundary controlled, have been determined by a numerical modal analysis. For an impact duration less than the Eigen period of the plate structure, the quasi-static load assumption is invalid and a transient analysis is required. For impact durations greater than the Eigen period, $t_{impact} \geq T_n$, impact loads on plates result in a boundary controlled response and a static analysis is adequate. The natural frequencies of the considered plate designs have been tabularized in *Table: 5-3*, allowing for comparison between the impact duration and Eigen period.

Plate Structure (7200x2875)	**Eigen Frequency [1/s]**	**Eigen Period [ms]**	**Plate response**
SPS 5-45-5	21,98	46	Boundary controlled
SPS 5-60-5	26,30	38	Boundary controlled
SPS 10-30-10	19,97	50	Boundary controlled
SPS 10-45-10	25,32	40	Boundary controlled
SSP 600	55,22	18	Boundary controlled

Table 5-3: The Eigen periods of plate structures (7200x2875) indicating an impact duration limit for which a static numerical analysis is adequate

The assumption of quasi-static loading is thus acceptable for all plate configurations even under the most conservative dropped impact duration of 60 *ms*. Hence, transient analyses are not required for any calculations made in this report.

Chapter 6

Conclusions & Recommendations

At the start of this research the following scope was set:

- *The scope of this research contains the assessment of impact behaviour on deck plating being subjected to dropped object loads to get a better understanding of plate design, the plate's impact response and maximum dissipated energy.*

In this chapter conclusions are drawn on whether SSP or SPS is the more optimal plate design type when subjected to dropped object impact loads, considering yield failure of rectangular areas at laydown area #7 of the Aasta Hansteen SPAR topside. Additionally, recommendations and requirements are set for further research.

6-1 Conclusions

The conclusions drawn from this research have been summarized into two sections. First the validity of the assumptions set prior to this study are confirmed or rejected. Subsequently conclusions are drawn with respect to SPS plate optimization.

6-1-1 Confirmation of set assumptions

Quasi-static impact load

From the comparison between impact durations and the structure's specific Eigen frequency it can be concluded that all dropped object impact cases considered in this report are governed by a boundary controlled impact response. Consequentially, only a single time frame during the impact duration is relevant for determining the maximum dissipated energy and thus a quasi-static impact load assumption is valid for both SSP and SPS structures.

Line vs. circular impact load

A difference in the considered loads applied to the structure result in different failure mechanisms, which as a consequence results in a different failure loads due to an increase in length over which hinge lines yield. For dropped impact loads, a circular failure mechanism was found which, for SPS in particular, requires a 3D analysis of the problem. A 2D analysis with the assumption of a line or point load has shown to be inconclusive, due to the circular failure mechanism for both types has proven to significantly increase the failure load. Thus, the assumption of a 2D case for SPS, similar to the one often used for SSP provides unreliable results and requires an overly complex analytical study.

Beam vs. Plate structure

For SSP-600 subjected to circular impact loads having a diameter slightly larger than the distance between 2 stiffeners only affects 2 stiffeners. Hence, no stiffeners other than the two closest to the location of impact need consideration. Thus, regardless of an increase in total width of the SSP plate, no additional energy dissipation is acquired. The assumption of a beam model having boundary constrains at only two opposite edges is therefore adequate.

In contrast to SSP, the increase of the plate's width for SPS is of great importance due to the additional stiffness acquired, as well as the deformation of the plate assuming a circular instead of double line yield failure mechanism.

6-1-2 SSP vs. SPS optimization

SSP-600 deflection limits energy dissipation

When yield failure of the plate structures (7200x2875) subjected to a circular impact load are considered the total dissipated energy limit is lowest for the SSP configuration. This is explained by the limited elastic deflection of this plate type. The SSP structure, due to its thickness, plastically deforms at a deformation of 12 mm, ultimately failing at 60 mm.

Optimal SPS design configuration

From the analyzed SPS configurations, SPS 5-45-5 has shown to provide a dissipated energy closest to the one found for SSP-600, having a maximum load resistance as well as having a stiffness in an acceptable range of the SSP-600 model. Although some greater SPS plate thicknesses provide greater dissipated energies than SSP, they also have higher masses and thus higher costs. An optimal SPS solution for low mass, high dissipated energy structures is found for low face plate to core thickness ratios. However, a minimum face plate and core thickness of 5 mm respectively 45 mm is required to provide greater load resistances than SSP-600, which ultimately results in higher mass plates.

SSP for beams, SPS for plates

A strong increase in the failure load (factor 3) is observed between SPS 5-45-5 (1200x2875) and SPS 5-45-5 (7200x2875). This is explained by the difference in failure mechanisms and the additional stiffness through boundary conditions along the short edges of the plate. In contrast, an increase in failure load of 20% has been found for SSP-600 (7200x2875) compared to SSP-600 (1200x2875). SSP provides a more resistant, lightweight solution when a beam structure is considered, while SPS 5-45-5 (7200x2875) provides better resistances when plates are considered.

Although the mass of the SPS 5-45-5 configuration is higher than the SSP-600 model, the greater deceleration distance provides additional energy to be dissipated and non-plastic deformations could prevent required replacement of the structure, saving costs.

6-2 Recommendations & further study

Further research on the subject of dropped object impact protection is required before implementation of SPS can be realized;

- **Experimental validation of the plate thickness design**
  Given the study's amount of variable parameters, validation of the considered plate configuration is required before implementation on the topside structure design. Besides validation, experimental research would provide additional data independent of data found Intelligent Engineering, increasing CB&I's trustworthiness to clients when offering this solution.
- **Investigate clamped boundary conditions**
  The additional stiffness the plates gains from clamped boundary conditions compared to the simply supported boundary conditions is disproportional to the standard bending formula for beams. The additional stiffness gained from these boundary conditions could prove SPS configurations with lower masses to be viable alternatives.
- **Core shear & indentation failure mode** While the yielding failure mode is governing for low velocity dropped object impacts, as a result of greater height drops core shear or indentation failure could be governing. With the yield failure load no longer being governing, it is essential to determine the failure loads of other failure modes.
- **Failure mode combinations** Especially for higher impact velocities, indentation could prove to be of such effect that the structures strength is compromised and the maximum yield failure load found is no longer valid. Instead, a reduced yielding failure load could be governing.
- **Cost evaluation of SSP compared to SPS**
  A relation between the costs and mass of SPS is more difficult to establish compared to other materials since a multitude of configurations is possible. A cost estimate of the plate itself could be provided by Intelligent Engineering. However, other savings as a result of easier replacement and installation costs may outweigh the costs of SSP and therefore need further evaluation.

Appendix A

Design parameters

This appendix provides the reader with the design parameters used for the impact analyses represented in a tabular overview.

Material Properties ***(S355; SSP & SPS face plates)***	**Symbol**	**Value**	**Units**
Yield stress	$\sigma_{y,fp}$	$355 \cdot 10^6$	Pa
Young's Modulus	E_{fp}	$2,1 \cdot 10^9$	Pa
Poisson Ratio	v_{fp}	$0,3$	$-$
Density	ρ_{fp}	7850	kg/m^3
Shear stress	τ_{fp}	$2,05 \cdot 10^8$	Pa
Shear modulus	G_{fp}	$8,08 \cdot 10^{10}$	Pa
Material Properties ***(polyurethane core)***	**Symbol**	**Value**	**Units**
Yield stress	$\sigma_{y,c}$	$16,1 \cdot 10^6$	Pa
Young's Modulus	E_c	$8,74 \cdot 10^8$	Pa
Poisson Ratio	v_c	$0,36$	$-$
Density	ρ_c	1050	kg/m^3
Shear stress	τ_c	$9,30 \cdot 10^6$	Pa
Shear modulus	G_c	$3,21 \cdot 10^8$	Pa
Dimensions of the structure ***(deck plating area # 7)***	**Symbol**	**Value**	**Units**
Stiffened Steel Plate span	L_{plate}	$7,2$	m
Stiffened Steel Plate width	W_{plate}	$2,875$	m
plate thickness	$t_{SSP,plate}$	10	mm
web thickness	$t_{SSP,web}$	190	mm
bulb thickness	$t_{SSP,bulb}$	25	mm
web width	$w_{SSP,web}$	10	mm
bulb width	$w_{SSP,bulb}$	40	mm
Sandwich Panel span	L_{plate}	$7,2$	m
Sandwich Panel width	W_{plate}	$2,875$	m
Face plate thickness	t_{fp}	≥ 10	mm
Core thickness	t_{core}	≥ 15	mm
Total thickness	t_{total}	≥ 25	mm
Dropped object parameters	**Symbol**	**Value**	**Units**
Kinetic Energy	E_k	$1,47 \cdot 10^3$	kJ
Dropped object mass	m_{do}	15.000	kg
Dropped object height	h_{do}	10	m
Dropped object impact velocity	v_{do}	$14,0$	m/s
Gravitational constant	g	$9,81$	m/s^2
Area of distributed loading	A_{do}	1	m^2

Appendix B

SPS Fabrication, Elastomer Material Properties and Fire Resistance

To prevent unforeseen risks, an introduction to the fabrication process, polyurethane material properties and fire resistance of SPS has been provided in this appendix. Research on these subjects were not in the scope of this project, but additional knowledge on these points is required before implementation of SPS is possible.

B-1 Fabrication Procedure SPS

The production and installation process provides insight in the practical limitations on the use of SPS in the offshore industry. The fabrication process of Sandwich Plate Systems is described in a 5-step overview.

1. The first step of fabricating SPS is the steel plates (face plates) undergoing a surface treatment via grit blasting. By grit blasting the surface of the face plate material is smoothened, a process required for the vulcanized bonding between the faceplate and the polyurethane later on during the process.

2. Perimeter bars are welded to the bottom faceplate and used to define the layout grid serving as the plate's boundaries (*Figure: B-1a*). Additionally they serve as the material to keep the face plates separated during the next phase of the fabrication process. Elastomer spacers are added to keep the face plates from taking an incorrect distance to the opposite face plate anywhere in the area of the layout grid (*Figure: B-1b*). The elastomer spacers are glued onto the steel plate instead of welded.

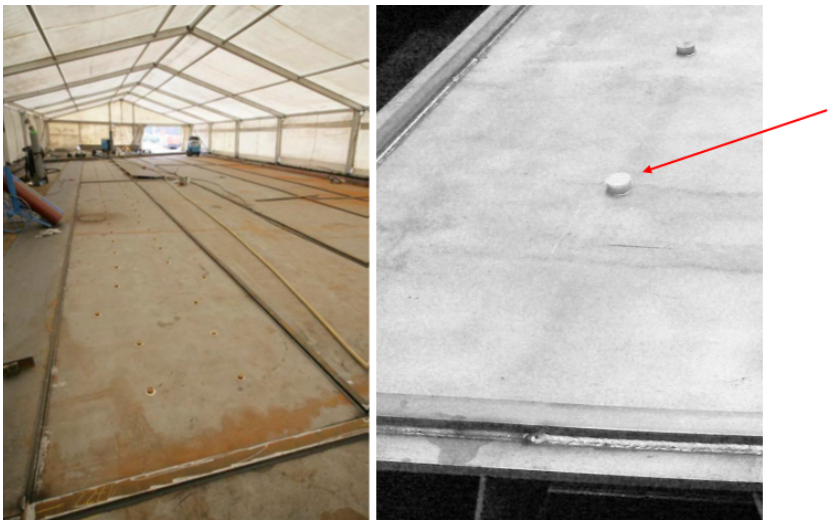

Figure B-1: (a) A layout grid has been prepared, the perimeter bars are welded and the elastomer spacers are glued onto the bottom steel faceplate. (b) Elastomer spacers to equal the space of the faceplates during installation - Source:

3. The second steel face plate is added on top of the perimeter bars and elastomer spacers (*Figure: B-2*). Again the face plate is glued to the elastomer spacers. The connection with the perimeter bars is made by a fillet weld. A cavity is now formed with the face plates and perimeter bars as boundaries.

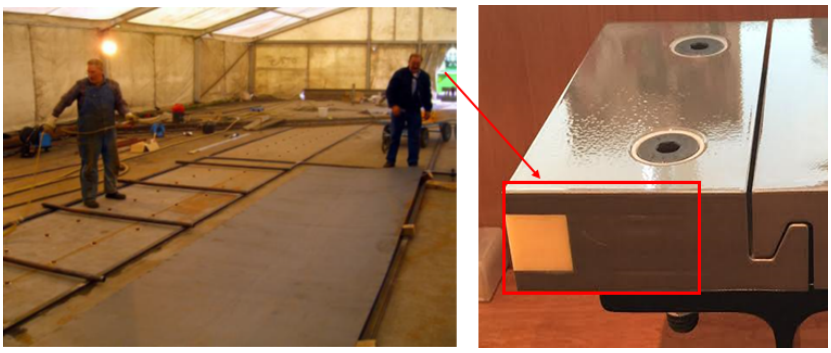

Figure B-2: (a) The top faceplate is placed on top of the perimeter bars/elastomer spacers. (b) Cross section of an SPS-panel; the perimeter bar used is highlighted [Source: SPS - Engineering Details, Intelligent Engineering Limited]

4. The top face plate is restrained by beams using magnetic clamps, preventing movement (*Figure B-3a*). By pre-drilled holes in the top face plate it is possible to inject the polyurethane into the cavity. Additional pre-drilled holes are used to enable the polyurethane from escaping the cavity when entirely filled, ensuring no air gaps are included (*Figure B-3b*).

Figure B-3: (a) Restraint beams are added to keep the top faceplate in place during pressurized injection. (b) Pre-drilled holes in the top faceplate enable the polyurethane from escaping the cavity when entirely filled. [Source: SPS - Engineering Details, Intelligent Engineering Limited]

5. After the entire cavity is filled the core must cure at room temperature for at least 48 hours. This enables the polyurethane to bind via adhesive (vulcanized) bonding to acquire its full bonding strength with the attached steel plate.

6. The pre-drilled holes are filled, leaving the polyurethane no longer directly exposed to the outside environment. Finally the magnetically clamped beams are removed and hoisting equipment is added allowing transportation of the Sandwich Plate Systems.

Overall, the production process duration is considerable and offshore production is not viable. In contrast to SSP, which can be partially replaced using welding techniques, the replacement of an SPS panel when plastically deformed does not seem straightforward as it requires full replacement of the panel.

B-2 Polyurethane material properties

Polyurethane, being a elastomer, has a strong temperature dependency. *Figure: B-4* indicates how the mechanical properties of polyurethane are effected by fluctuations in temperature.

Mechanical Properties

Tensile Behaviour

Property	-80°C	-60 °C	-40 °C	-20 °C	23 °C	60 °C	80 °C
E (MPa)	3859	2924	1765	1164	874	436	248
σ_y (MPa)	38.9	29.5	28.4	23.0	16.1	8.1	6.2
ε_u (%)	7.2	11.1	13.2	15.1	32.1	43.1	47.4

Compressive Behaviour

Property	-80°C	-60 °C	-40 °C	-20 °C	23 °C	60 °C	80 °C
E (MPa)	3878	2813	1347	1166	765	501	336
σ_y (MPa)	52.1	33.5	30.9	21.4	18.0	10.2	7.9

Shear Modulus (Torsion Pendulum Test)

Property	-80°C	-60 °C	-40 °C	-20 °C	23 °C	60 °C	80 °C
G (MPa)	1386	955	559	429	285	180	135

Thermal Properties

Thermal Expansion Coefficient

Property	-30 °C	-10 °C	10 °C	30 °C	50 °C	70 °C
α ($x10^{-6}$m/m·°C)	96.1	120.1	133.6	148.7	162.5	184.7

Specific Heat

Property	-20 °C	23 °C	60 °C	80 °C
c (J/kg·°C)	1217	1414	1588	1687

Thermal Conductivity

k = 0.1774 W/m•°C (R-value/mm thickness = 0.032 °F·ft^2·h/Btu)

Figure B-4: The dependency of material properties of Polyurethane on the temperature [Source: SPS - Engineering Details, Intelligent Engineering Limited]

The influence of the temperature on the material properties of Polyurethane is insignificant for the yielding failure load, as the steel face plates offer the primary part of the load carrying capacity and maximum strains in the core are not exceeded under plastic deformation of the steel face plates. Additionally, it has been assumed the structure's temperature does not increase during impact and the structure does not experience strong varying temperatures during operation.

B-3 Fire Safety of SPS

Previous research on fire safety and heat resistance has been conducted by Intelligent Engineering *[3]*. To determine the insulation effectiveness and to check if the safety requirements are met, 1 and 2 hour fire tests were carried out. Distinction was made between direct and indirect exposure to the polyurethane core material at a temperature of 945C.

B-3-1 Indirect exposure

According to Intelligent Engineering, during indirect exposure to fire, the thickness from the elastomer core acts as an effective insulator against heat transfer. A comparison between SSP and SPS has been conducted by Intelligent Engineering, where both plate structures were exposed to an indirect fire test. *Table: B-1* shows the difference in maximum surface temperature of the unexposed plate sides after a 1 hour fire test at 945 C.

Plate Type	Plate Thickness [mm]	Exposure duration	Fire protection coating	Temperature of unexposed surface
SPS	4-25-4	1 hour	No	138 C
SPS	4-20-4	1 hour	No	209 C
SSP	5	1 hour	No	713 C
SSP	5	1 hour	50 [mm] wool board	192 C

Table B-1: The surface temperature of the unexposed side of SPS structures and stiffened steel plates after a 1 hour first test at 945C [Source: SPS - Engineering Details, Intelligent Engineering Limited]

For this specific case, SPS offers a better fire protection than stiffened steel plates through their additional thickness and reasonable polyurethane insulator. Additionally, the SPS plate retained its full composite structural integrity, as long as the steel plate did not melt.

Although the by SPS provided fire resistance suffices the rules and regulations, a comparison between both SSP and SPS structures has not been conducted for plates of similar stiffness. In order to conclude to which extent SPS offers improved fire resistance, additional tests are required.

B-3-2 Direct exposure

Polyurethane, as a thermosetting polymer, does not have a melting point. The core material of SPS will therefore act like a sacrificial layer when directly exposed to a fire. In case the Polyurethane is exposed and a sufficient heat level is reached, the core material starts to burn and develop toxic smoke composed of carbon monoxide, hydrogen cyanide and nitrogen oxides.

Direct exposure fire tests have been conducted by Lloyd's Register in accordance with IMO guidelines, indicating SPS panels can be considered better or equivalent to stiffened steel plates with a A-60 fire rating. During these tests developed toxics did not exceed the specified toxicity limits. Further research on direct fire exposure is thus not required *[3]*.

Appendix C

Verification Study

Verification of both the SSP and SPS models are executed to check whether the FEA was conducted properly. The numerical model's shape, material parameters and failure mechanism are verified by determining the elastic and plastic section moduli, as well as the force-deflection curves. Boundary conditions and loads have been applied in a way such that they accurately represent the analytical case. An element convergence study has been conducted in order to find the most convenient mesh density.

C-1 Model verification SSP

To verify the numerical SS-P600 model, a single hinge failure mechanism, similar to the analytical case, has been ensured. To do so, a line deflection has been applied at the middle of the plate and both stiffeners have been restricted from moving in transverse direction. Element convergence has been accounted for by choosing a high density mesh with elements of $0,04$ *mm*.

The normal stresses in longitudinal direction for a single hinge failure mechanism are shown in *Figure: C-1*. The stresses at the middle of the span, at the bulb's outer elements, have been used to determine the elastic and plastic section moduli of the SSP-600 model.

The difference between the analytical- and numerical section moduli are tabularized in *Table: C-1*. The negligible errors indicate the boundary conditions, material properties and structure's shape have been accurately modeled. The differences are explained by imperfect modeling of the bulb and the conservative choice made for the effective width during the analytical study.

The extent to which the difference in elastic section moduli can be contributed to the effective width has been determined. Models with a stiffener interval distance $\Delta w_{stiffeners}$, in the range of 100 to 650 *mm*, have been researched. For a single hinge line failure mechanism, the influence of the effective width on the elastic section modulus is displayed in *Figure: C-2*.

Elastic longitudinal normal stress in the SSP-600 model

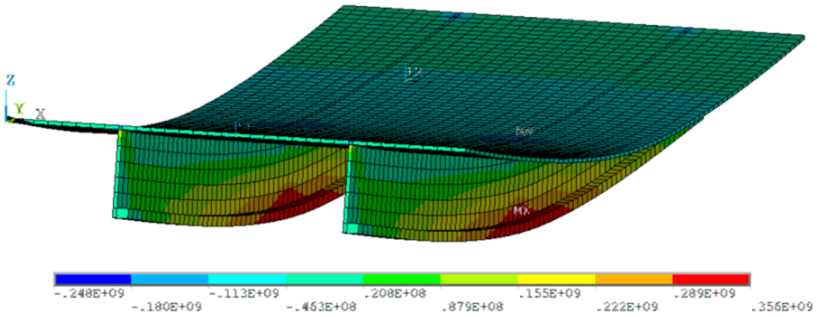

Figure C-1: Elastic longitudinal normal stress in the SSP600 (1200x2875) when subjected to point deflections

Section Modulus	Analytical $[m^3]$	Numerical $[m^3]$	Error [-]
Elastic	$2,82 \cdot 10^{-4}$	$2,89 \cdot 10^{-4}$	$\leq 1\%$
Plastic	$4,02 \cdot 10^{-4}$	$4,05 \cdot 10^{-4}$	$\leq 1\%$

Table C-1: The difference between the analytical and numerical section moduli for SSP600 (1200x2875)

Influence of the stiffener interval distance on the elastic section modulus

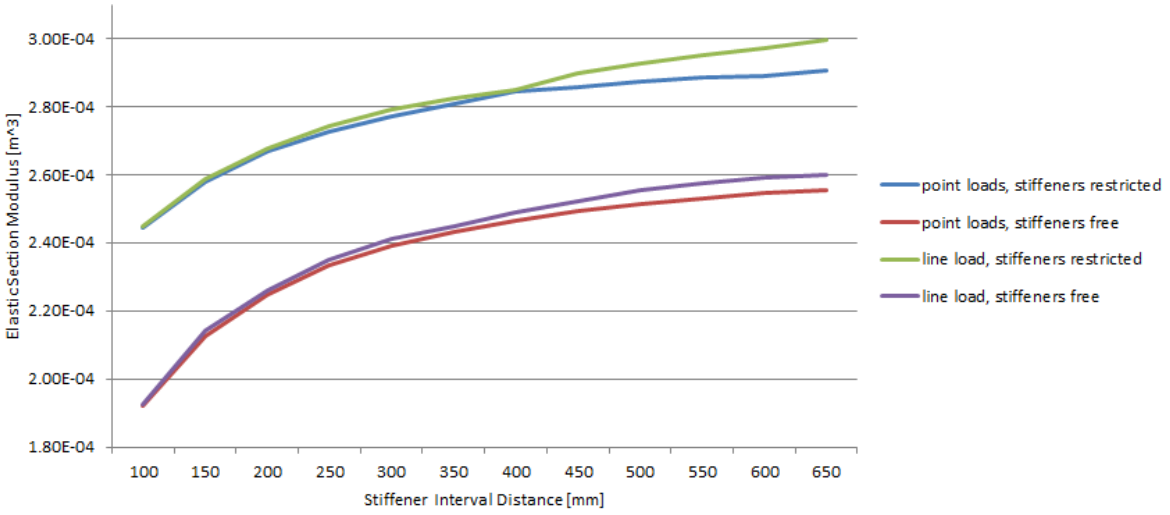

Figure C-2: The influence of the stiffener interval distance on the elastic section modulus of SSP (1200x2875)

For the SSP model with the stiffeners restricted, a maximum value of the elastic section modulus per stiffener of $W_{e,SSP} = 2,9 \cdot 10^{-4}\ m^3$ is found at an interval distance $\Delta w_{stiffeners} = 600\ mm$. The previously chosen effective width of 420 mm with an elastic section modulus of $W_{e,SSP} = 2,82 \cdot 10^{-4}\ m^3$ could be considered conservative and explains the difference between the analytical and numerical case. The effective width for models where the stiffeners are considered free is found at similar interval distance.

CB&I has chosen the initial design distance between each stiffener as a minimal bending stiffness requirement with a minimal mass, see *Figure C-3*. For a larger distances the minimal

stiffness is exceeded while for smaller distances the minimum mass is increased.

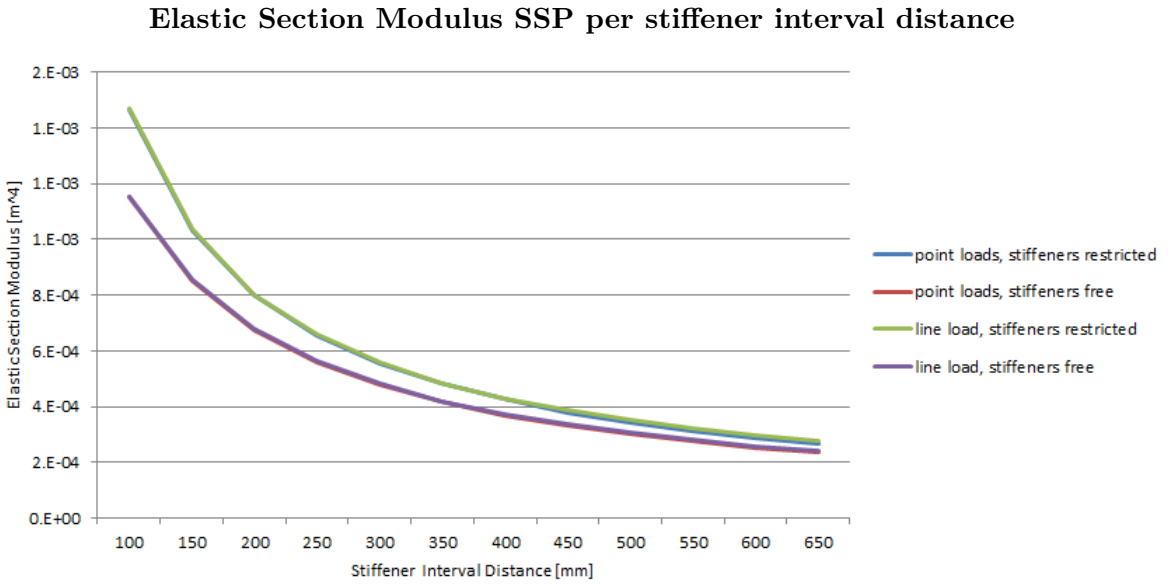

Figure C-3: The elastic section modulus of SSP (1200x2875) as a function of the stiffener interval distance

The numerically found plastic section moduli are determined using force-deflection diagrams. Distinction is made between an applied line deflection and point deflections, to determine whether local deformation effects are of influence. The elements at which first plastic deformation is expected have been monitored and compared to the total reaction force at the boundaries. The force-deflection curve for SSP600 (1200x2875) is shown in *Figure C-4*.

The difference in point and line deflection has shown neglectable for the failure load of the SSP600 structure. With a failure load at $F_{failure} = 405\ kN$, the plastic section modulus is in good agreement with the analytically found value.

Model (1200x2875)	Analytical failure load [N]	Numerical failure load [N]	Error [-]
SSP600 Line deflection	397.106	405.500	$\leq 2\%$
SSP600 Point deflection	397.106	402.375	$\leq 2\%$

Table C-2: Comparison of the analytical and numerical failure loads for the SSP600 beam configuration (1200x2875)

C-2 Model verification SPS

C-2-1 SPS (50x2875)

The analytical SPS model has been verified by applying a line deflection along the width at the middle of the a SPS beam structure. To realize a 2D-approximation, a width of 50 mm has been chosen for the numerical models, *Figure: C-5*.

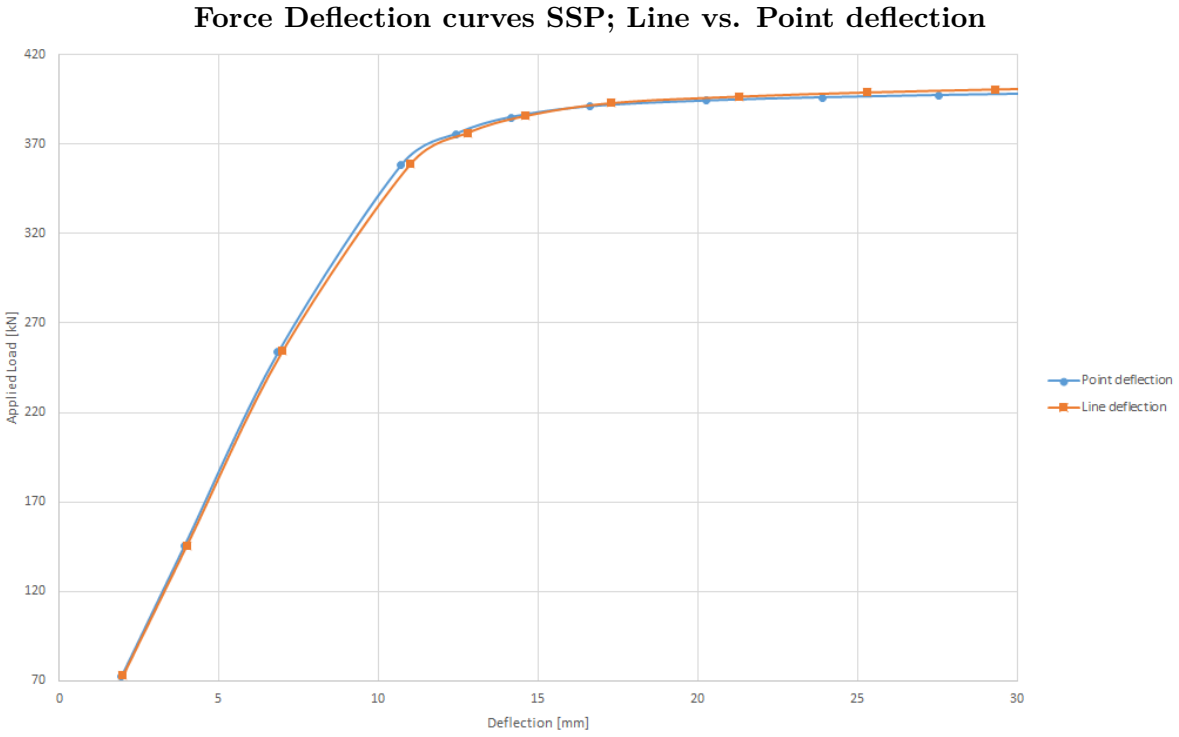

Figure C-4: The force-deflection curve for SSP600 (1200x2875) when subjected to point and line deflections

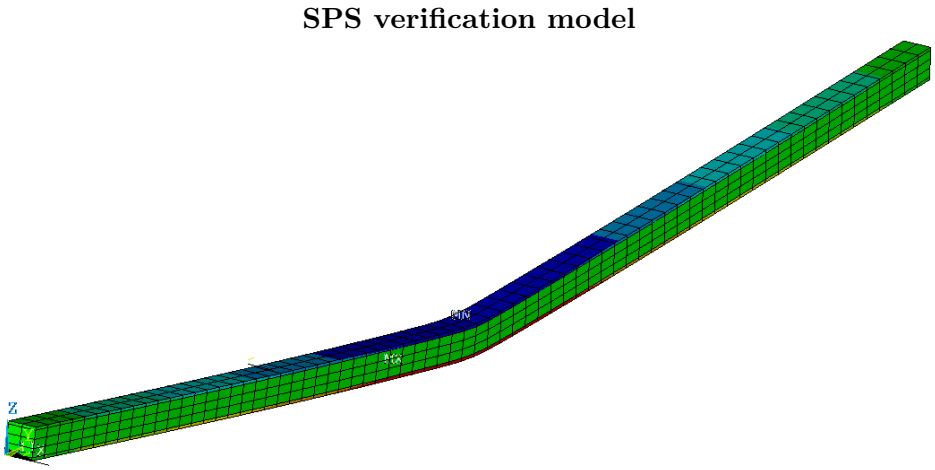

Figure C-5: Verification model SPS 5-45-5 (50x2875)

The analytical failure load values determined in *Chapter:3* have been compared to the numerical failure loads. The failure loads for models with thicknesses, 5-15-5, 5-30-5, 5-45-5 and 5-60-5 *mm* have been determined from the Force-Deflection curves associated with each model, *Figure: C-6*. Here, for the initial linear part of the curves the deflection is elastic, The second linear part, which is not denoted clearly in this particular figure, is the elasto-plastic deformation where the face plates experience plasticity, while the core remains elastic. The third part of the curve, where a slight increase of the failure load is mainly found for greater

core thicknesses, is realized through the remaining yield stress in the core. The additional load from this stress has not been considered analytically, which is why numerically the failure load has been considered at the 'knee' of the force-deflection curve.

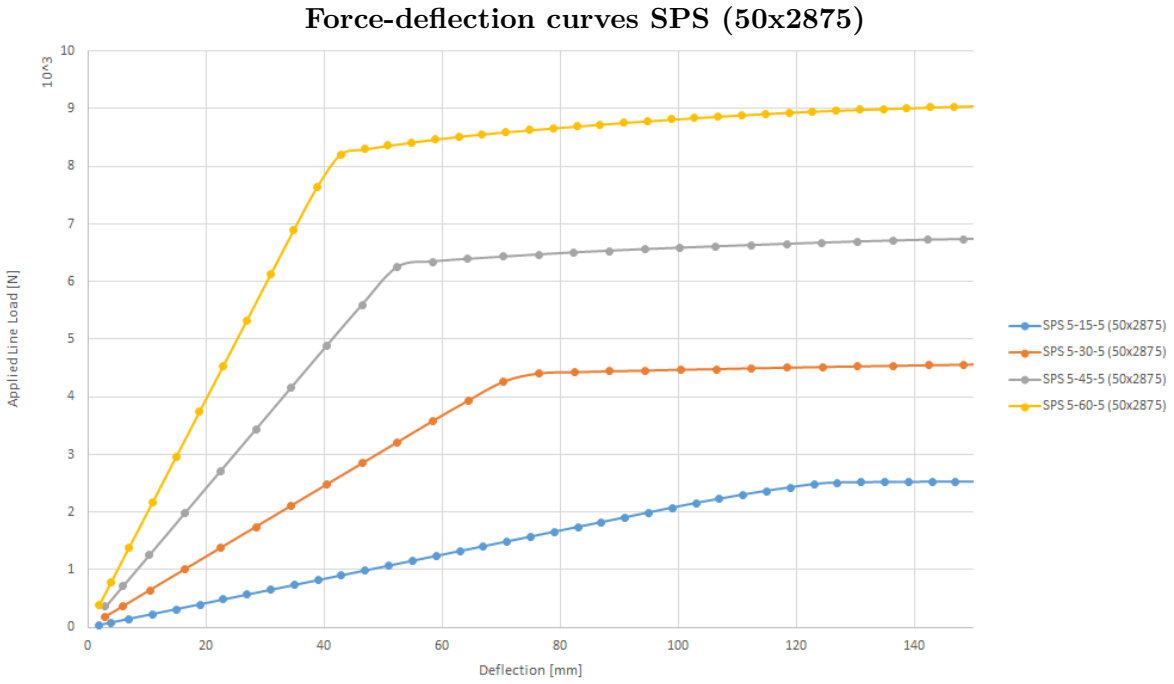

Figure C-6: Force-Deflection curves for SPS beam verification models (50x2875)

Table C-3 provides a comparison between analytical and numerical found values for the failure load. As a whole the model and the applied boundaries, as well as the line deflection can be considered to provide accurate results for the beam assumption of the SSP and SPS beams.

Model	Analytical failure load [N]	Numerical failure load [N]	Error [-]
SPS 5-15-5 (50x2875)	2.498	2.545	$\leq 2\%$
SPS 5-30-5 (50x2875)	4.321	4.406	$\leq 2\%$
SPS 5-45-5 (50x2875)	6.173	6.205	$\leq 1\%$
SPS 5-60-5 (50x2875)	8.026	8.211	$\leq 3\%$

Table C-3: Comparison of the analytical and numerical failure loads for various SPS beam configurations (50x2875)

C-2-2 SPS (1200x2875)

For the SPS (1200x2875) cases, a similar approach is used. However, due to the width of the plate, the Poisson ratio has to be considered.

Taking into account the Possion ratio ν, *Table: C-4* provides the accuracy of the analytical beam- versus plate model assumption.

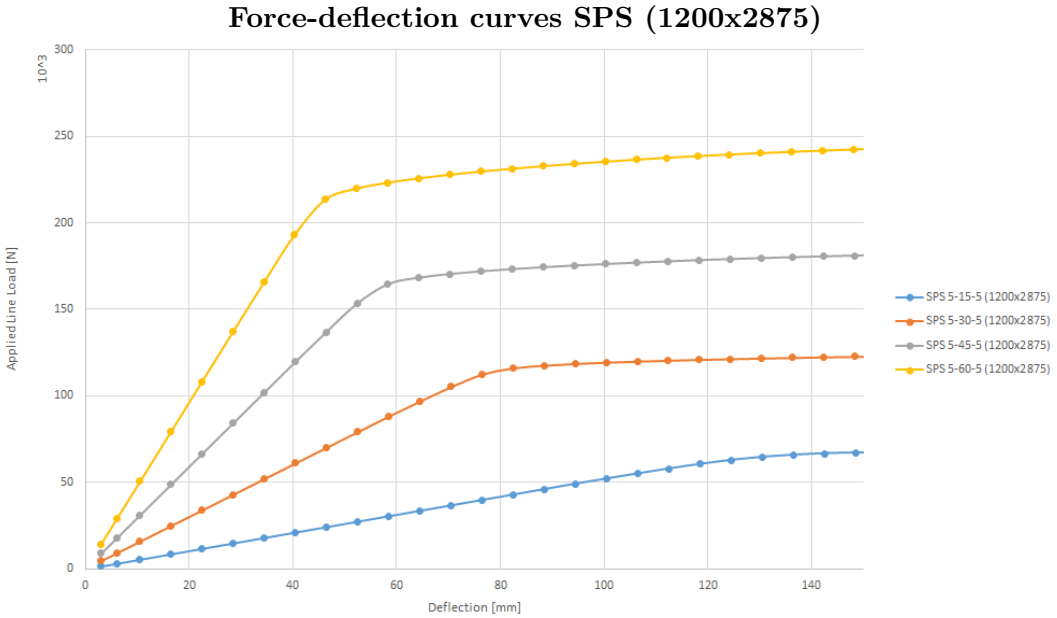

Figure C-7: Force deflection curves for various SPS configurations (1200x2875)

Model (1200x2875)	Analytical failure load [N]	Numerical failure load [N]	Error excl. Poisson	Error incl. Poisson
SPS 5-15-5	59.952	69.469	$\leq 15\%$	$\leq 5\%$
SPS 5-30-5	103.704	116.049	$\leq 11\%$	$\leq 2\%$
SPS 5-45-5	148.173	185.916	$\leq 25\%$	$\leq 14\%$
SPS 5-60-5	192.624	249.500	$\leq 29\%$	$\leq 18\%$

Table C-4: Comparison of the analytical and numerical failure loads for various SPS beam configurations (1200x2875)

C-3 Element Convergence study

To complete the verification of the models, an element convergence study has been conducted. The convergence study provides insight on how results at the same point and time instance are affected by the model's element size. Due to the second order convergence dependency of elements with respect to the stresses, the longitudinal normal stresses in the verification models subjected to a line deflection have been measured during their elasto-plastic phase.

For converging analyses, a finer mesh (1/h) provides a continuously decreasing error for the found results (E) and one may conclude the model's results to be mesh density independent for any denser meshes, *Figure: C-8*. However, convergence of the results for static structural analyses is often found for relatively low density meshes and therefore a minimum percentage error is chosen instead, as a limitation on the minimum mesh density. For such cases a mesh density beyond the highest possible mesh density of the used computer system/program is expected to not provide more accurate results. Any mesh density with an error less than or equal to 1% of the result found for the highest density mesh is then assumed acceptable.

For the SSP and SPS models an element convergence study has been conducted for element

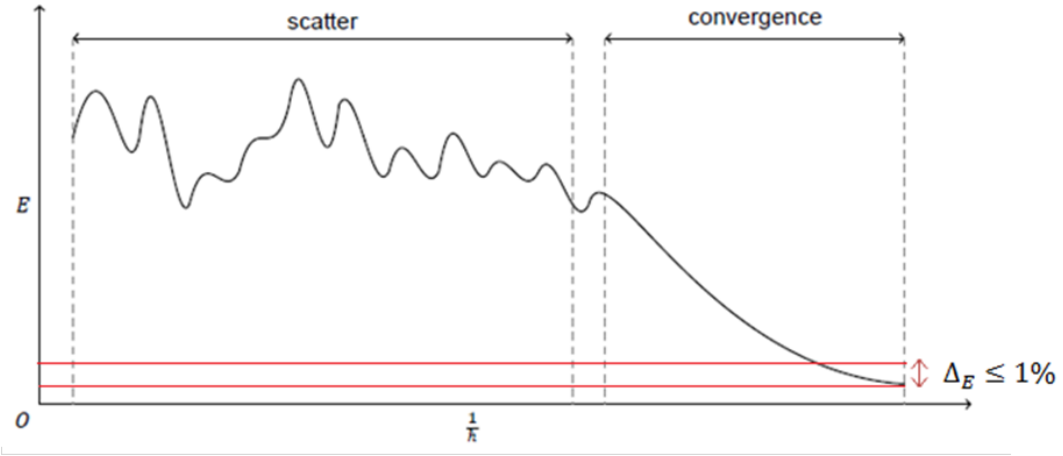

Figure C-8: Universal element convergence graph

sizes of 2 to 16 [cm] with 2 [cm] size intervals. The minimum element size of 2 and 4 [cm] for SSP and SPS respectively is limited by the maximum amount of nodes allowed by ANSYS. The maximum element size of 16 cm is chosen as a maximum limit to prevent shape size warnings. Due to model symmetry single element inspection at the point of plastic deformation is assumed sufficient.

C-3-1 Element convergence study; SSP600

In order to find the optimal mesh density for the SSP600 beam model, the results and computation time for plastic analyses have been monitored. The mesh density and analyses' computation time have been summarized in *Table: C-5*.

Element size [mm]	Element layout [L*W*T]	Amount of elements	Computation time [s]
16	18*(10*1+2*4)	324	21
14	21*(14*1+2*4)	462	32
12	24*(14*1+2*4)	528	36
10	29*(14*1+2*4)	638	45
8	36*(18*1+2*5)	1008	71
6	48*(22*1+2*6)	1632	123
4	75*(34*1+2*7)	3456	285
2	144*(62*1+2*16)	13536	1416

Table C-5: Mesh density and calculation time for plastic deformations of SSP600 (1200x2875))

In *Figure: C-9* the longitudinal normal stresses in the SSP600(1200x2875) at the outer element of the bulb have been plotted versus the deflection at the middle of the plate. The model convergences with continuously increasing accuracy of results for elements smaller than 10 [mm]. Although the error between the stresses are less than or equal to 2% at full hinge formation for all element sizes, the stresses vary significantly during the elastic and elasto-plastic phase. Therefore, only elements smaller than 10 [mm] have been considered to provide acceptable results.

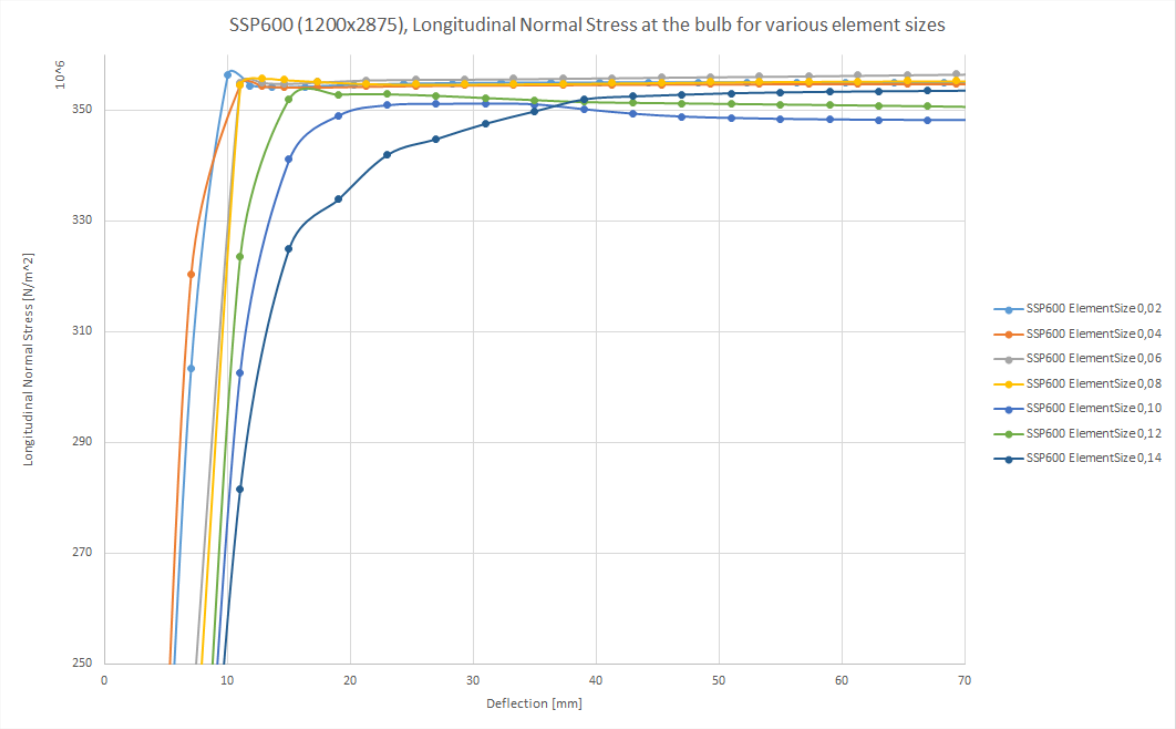

Figure C-9: Longitudinal Normal Stress at the bulb of the SSP600 (1200x2875) model when subjected to a line deflection

Taking into account the accuracy of the results, as well as the computation time required to execute the analyses, elements of size 4 [mm] have been considered optimal for the SSP600 models.

C-3-2 Element convergence study; SPS 5-15-5

The optimal mesh density for SPS has been conducted based on the thin SPS; 5-15-5 (1200x2875) model. The required mesh density is highest for this model, as its low core thickness leads to element shape limit warnings for elements equal or greater than 12 [mm]. Although hourglassing did not occur and full integration was not required for these element sizes, flawed results could be expected for these element sizes, for that reason they have not been considered viable. *Table: C-6* provides an overview of the studied mesh densities and their associated computation times.

The longitudinal normal stresses associated with the line deflection for each element size have been presented in *Figure: C-10*. Elements with a size of 8 [mm] are optimal when taking into account the computation time and error found for the different mesh densities. The error has been deteremined from the highest mesh density with elements of size 4 [mm], *Table:C-7*.

Element size [mm]	Element layout [L*W*T]	Amount of elements	Computation time [s]
16	18*8*5	720	64
14	21*10*5	1050	95
12	24*10*5	1200	113
10	29*12*5	1740	170
8	36*16*5	2880	319
6	48*20*5	4800	646
4	72*30*5	10800	1883
2	144*60*5	43200	-

Table C-6: Mesh density and calculation time for plastic deformations of SPS 5-15-5 (1200x2875))

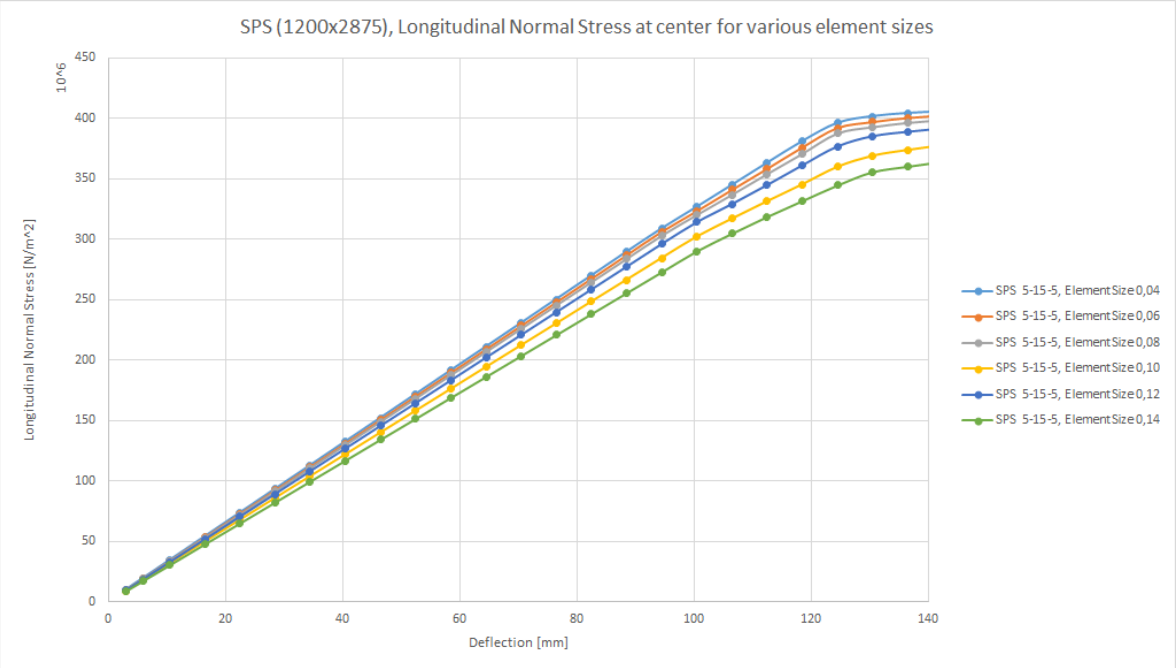

Figure C-10: Longitudinal Normal Stress at plastic initiation for the SPS 5-15-5 (1200x2875) model when subjected to a line deflection

Element size [mm]	Longitudina Normal Stress $[N/m^2]$	Error
4	$410 \cdot 10^6$	-
6	$409 \cdot 10^6$	$\leq 1\%$
8	$408 \cdot 10^6$	$\leq 1\%$
10	$399 \cdot 10^6$	$\leq 3\%$
12	$404 \cdot 10^6$	$\leq 2\%$
14	$392 \cdot 10^6$	$\leq 4\%$

Table C-7: Longitudinal Normal Stresses for various element sizes of SPS 5-15-5 (1200x2875)) model

Appendix D

Validation ANSYS

Validation, which is often conducted via experiments, is key in finding the reliability of the results. More complex models require validation instead of verification, as calculations of these by hand are too time consuming.

In general, experiments are the preferred validation method but due to time and financial restrictions other validation methods are sought for. Making use of previous research by comparing already published data with the research conducted in this report could be a viable alternative. However, previous research is limited to beam structures or plates with dimensions other than those considered here.

Measurements of dropped impact experiments have been conducted by Intelligent Engineering. The results they found between the static and dynamic impact strength of a specific SPS configuration is shown in *Figure D-1*.

The figure indicates the conducted static analysis followed a similar trend to the dynamic analysis, which included strain rate effects and plate delamination. The static analysis thus gives a relatively good indication of the energy absorption for the loading conditions considered in this report.

Further validation of the numerical is recommended.

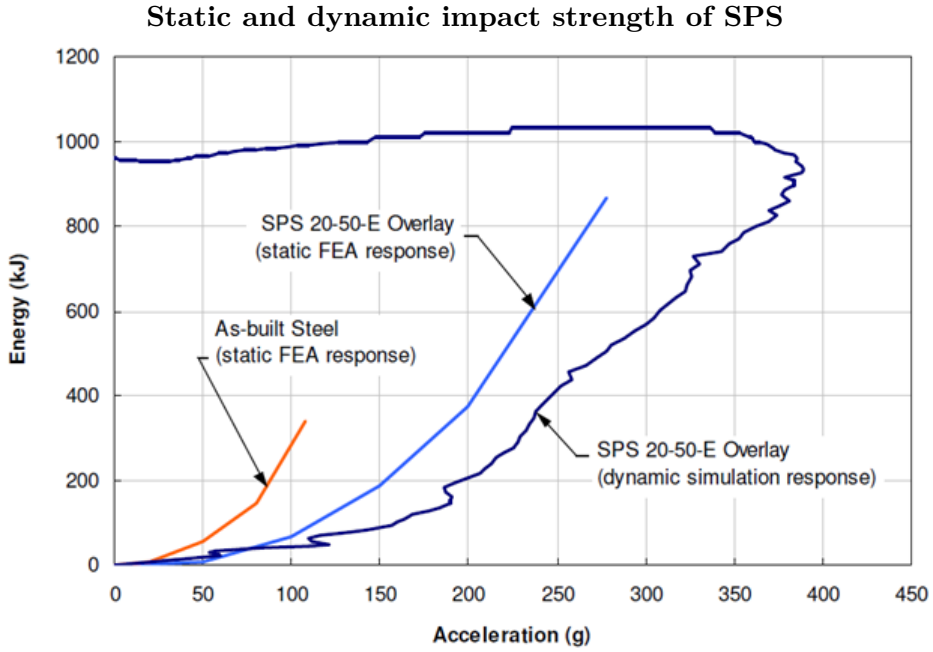

Figure D-1: The dissipated energy plotted versus the acceleration of an SPS plate for static and dynamic calculations when subjected to circular impact loads

Bibliography

[1] *Intelligent Engineering - Project Portfolio.* Intelligent Engineering (UK) limited, 2016.

[2] *Intelligent Engineering; Technical Note - SPS Behaviour under impact loads.* Intelligent Engineering (UK) limited, 2009.

[3] *Intelligent Engineering; Technical Note - Fire Resistance of SPS.* Intelligent Engineering (UK) limited, 2010.

[4] F. J. Plantema, *Sandwich construction.* Wiley, New York, 1966.

[5] H. G. Allen, *Analysis and design of structural sandwich panels.* Elsevier, 2013.

[6] D. Zenkert, *An introduction to sandwich construction.* Engineering Materials Advisory Services, 1995.

[7] T. C. Triantafillou and L. J. Gibson, "Failure mode maps for foam core sandwich beams," *Materials Science and Engineering*, vol. 95, pp. 37–53, 1987.

[8] A. Vrouwenvelder, "The plastic behaviour and the calculation of beams and frames subjected to bending," *Technical University Delft; Lecture book*, 2003.

[9] Y. Yuan and P. Tan, "Deformation and failure of rectangular plates subjected to impulsive loadings," *International Journal of Impact Engineering*, vol. 59, pp. 46–59, 2013.

[10] N. Razali, M. Sultan, F. Mustapha, N. Yidris, and M. Ishak, "Impact damage on composite structures – a review," *The International Journal Of Engineering And Science*, vol. 3, p. 7, 2014.

[11] C. A. Steeves and N. A. Fleck, "Collapse mechanisms of sandwich beams with composite faces and a foam core, loaded in three-point bending. part i: analytical models and minimum weight design," *International Journal of Mechanical Sciences*, vol. 46, no. 4, pp. 561–583, 2004.

[12] S. Teixeira de Freitas, *Steel plate reinforcement of orthotropic bridge decks.* Delft University of Technology, 2012.

[13] *DNV: RP C-208 - Determination of Structural Capacity by Non-linear FE analysis Methods.* DNV AS, 2013.

[14] *Intelligent Engineering; SPS - Engineering Details.* Intelligent Engineering (UK) limited, 2003.

[15] *DNV: RP C204 - Design Against Accidental Loads.* DNV AS, 2004.

[16] *Lloyd's - Provisional Rules for the Application of Sandwich Panel Construction to Ship Structure.* Lloyd's Register, 2006.

Bibliography

[1] *Intelligent Engineering - Project Portfolio.* Intelligent Engineering (UK) limited, 2016.

[2] *Intelligent Engineering; Technical Note - SPS Behaviour under impact loads.* Intelligent Engineering (UK) limited, 2009.

[3] *Intelligent Engineering; Technical Note - Fire Resistance of SPS.* Intelligent Engineering (UK) limited, 2010.

[4] F. J. Plantema, *Sandwich construction.* Wiley, New York, 1966.

[5] H. G. Allen, *Analysis and design of structural sandwich panels.* Elsevier, 2013.

[6] D. Zenkert, *An introduction to sandwich construction.* Engineering Materials Advisory Services, 1995.

[7] T. C. Triantafillou and L. J. Gibson, "Failure mode maps for foam core sandwich beams," *Materials Science and Engineering*, vol. 95, pp. 37–53, 1987.

[8] A. Vrouwenvelder, "The plastic behaviour and the calculation of beams and frames subjected to bending," *Technical University Delft; Lecture book*, 2003.

[9] Y. Yuan and P. Tan, "Deformation and failure of rectangular plates subjected to impulsive loadings," *International Journal of Impact Engineering*, vol. 59, pp. 46–59, 2013.

[10] N. Razali, M. Sultan, F. Mustapha, N. Yidris, and M. Ishak, "Impact damage on composite structures – a review," *The International Journal Of Engineering And Science*, vol. 3, p. 7, 2014.

[11] C. A. Steeves and N. A. Fleck, "Collapse mechanisms of sandwich beams with composite faces and a foam core, loaded in three-point bending. part i: analytical models and minimum weight design," *International Journal of Mechanical Sciences*, vol. 46, no. 4, pp. 561–583, 2004.

[12] S. Teixeira de Freitas, *Steel plate reinforcement of orthotropic bridge decks.* Delft University of Technology, 2012.

[13] *DNV: RP C-208 - Determination of Structural Capacity by Non-linear FE analysis Methods.* DNV AS, 2013.

[14] *Intelligent Engineering; SPS - Engineering Details.* Intelligent Engineering (UK) limited, 2003.

[15] *DNV: RP C204 - Design Against Accidental Loads.* DNV AS, 2004.

[16] *Lloyd's - Provisional Rules for the Application of Sandwich Panel Construction to Ship Structure.* Lloyd's Register, 2006.